BLANK PAGE

6453-6012-KU-000

BSD-TR-64-342

TURBULENT DIFFUSION OF A REACTING WAKE

By W. H. Webb and L. A. Hromas

30 JANUARY 1964
REVISED 3 DECEMBER 1964

Contract No. AF 04(694)-440

Prepared for
HQ BALLISTIC SYSTEMS DIVISION
AIR FORCE SYSTEMS COMMAND
UNITED STATES AIR FORCE
Norton Air Force Base, California

TRW SPACE TECHNOLOGY LABORATORIES
THOMPSON RAMO WOOLDRIDGE INC.

ERRATA

Page	Correction
iii	Appendix.....p. 28 References.....p. 25
iv	Fig. No. Page 1.....30 2.....31 3.....32 4.....33 5.....34 6.....35 7.....36 8.....37 9A.....38 9B.....39 10.....40 11A.....41 11B.....42

BSD-TR-64-342

TURBULENT DIFFUSION OF A REACTING WAKE

by

Wilmot H. Webb
and
Leslie A. Hromas

TRW Space Technology Laboratories
Redondo Beach, California

Contract No. AF 04(694)-440

Presented at AIAA Annual Meeting
30 January 1964

Revised 3 December 1964

Prepared for

HEADQUARTERS
BALLISTIC SYSTEMS DIVISION
AIR FORCE SYSTEMS COMMAND
UNITED STATES AIR FORCE
Norton AFB, California

ABSTRACT

Properties of the nonequilibrium hypersonic turbulent wake have been calculated from an integral solution for the coupled diffusion of mass and energy. Emphasis is placed on:

1) A comparison of a slender body calculation from the present simple method with results obtained for the same case by more advanced mathematical techniques such as finite difference methods

2) New blunt body results in which the reacting inviscid flow is entrained by the turbulent inner wake

3) The effect of contaminants on both slender and blunt body wakes

4) A comparison of the present calculations with ballistic range measurements for wake velocity and electron density.

The analysis described herein is a direct extension of the method proposed by Lees and Hromas for the equilibrium wake. By using two parameters to describe the distribution of each species in the wake, the integral method applied here provides sufficient generality to permit the determination of a variety of reacting turbulent flow fields, yet retains the basic numerical simplicity inherent in integral techniques. In the chemical kinetic model studied, particular attention is paid to the processes of far downstream electron decay, and for the first time combined atomic and molecular oxygen attachment, charge neutralization, and charge exchange reactions are considered. In addition, some new explicit solutions are given which provide useful criteria in evaluating the respective roles of chemical reactions and diffusion in the wake. These solutions are useful in obtaining scaling laws which are not always evident in detailed computer calculations.

CONTENTS

ILLUSTRATIONS

NOMENCLATURE

$B(x)$	$\dfrac{h(0,x) - h_f(x)}{h_\infty}$
C_D	Wake drag coefficient
d	Body diameter
g	Inviscid enthalpy radial distribution function
G	Turbulent radial distribution function
h	Thermal and chemical enthalpy
H	$h_L(0)/h_\infty - 1$
H_s	Free stream stagnation enthalpy
k	Reaction rate
K	Universal diffusion constant
m	Two dimensional ($m = 0$) or axi-symmetric ($m = 1$) exponent
M	Mach number
$\mathcal{M}$	Molecular weight
n_i	Species number density
p	Pressure
R_o	Gas constant
T	Temperature
u	Axial velocity
v	Radial velocity
x	Axial coordinate
y	Radial coordinate
Y	Howarth-Dorodnitsyn scale
a_i	Species mass fraction
β_i	$\left[a_i(0,x) - a_{i_f}\right] \Big/ \left[a_{i_o} - a_{i_f}\right]$

γ_∞	Specific heat ratio
ϵ	Turbulent diffusivity
ρ	Density
θ_i	Y_T/Y_{s_i}
$\dot{\omega}_i$	Species production term, $d(\alpha_i\rho)/dt$

Subscripts

A	Refers to atomic species
a	Attachment rate
b	Backward reaction rate
e	Refers to electrons
E	Equilibrium value
f	Denotes edge of wake; also forward reaction rate
i	Denotes i^{th} species
L	Inviscid flow quantity
o	Quantity at wake origin ($x = x_o$)
r	Recombination rate
s	Species quantity
T	Turbulent flow quantity
∞	Free stream value

INTRODUCTION

The trails behind meteors entering the atmosphere have long been of interest to astronomical observers.[1] Recently, new emphasis has been placed on the analysis of re-entry wakes due to the problems of detection of, and communication with, military and space vehicles. Over a major portion of an atmospheric re-entry flight, the wake is turbulent. At present a number of analyses of the chemically frozen or equilibrium wake are available. For example, References 2 and 3 treat the case where the enthalpy in the external stream is uniform, while References 4 and 5 take into account the entrainment of vorticity in the external flow by the growth of the turbulent core.

However, chemical equilibrium prevails over only the very lowest part of the re-entry trajectory, thus more recent attention has been given to the reacting turbulent wake. Initially, Lees[6] gave a simple integral solution for electron concentration in the flow, with a given temperature distribution. Next, Bloom and Steiger[7] reported some early results of an integral solution for the nonequilibrium laminar and turbulent wake of a slender body. A single parameter was used to represent each chemical species and the species radial distribution was related to the velocity distribution (Crocco relation).

A simple version of the technique used herein was then given by the present authors in Reference 8, where sample calculations were presented for the wake of a slender body. The present work extends these early results to blunt body flows and includes results for the contaminated wakes of both blunt and slender bodies. In addition, comparisons with ballistic range measurements of wake velocity and electron concentration and comparisons with detailed finite difference calculations of other workers are also given.

In an analysis subsequent to References 1 through 8, Lien, Erdos and Pallone[9] have applied a refined integral method for slender bodies in which both the momentum and species equations are employed as well as the energy equation. Wake axis values of the flow variables and a profile shape factor are used as parameters, and, as in the original Lees-Hromas

method and its present extension, integrated conservation equations along with the axis equations are then used to evaluate the parameters. In the method of Lien, et al., the wake width in Howarth-Dorodnitsyn coordinates is assumed to be given. The advantage of this refined solution for the turbulent wake over the present approach is in the inclusion of a variable velocity which is important in the first 0 to 10 diameters. On the other hand, the present approach does not require an empirical wake growth and allows for a radial variation in inviscid enthalpy.* Reference 9 also gives a nonequilibrium analysis for the laminar wake using a strip method where five strips are usually used (one "strip" is used in the usual integral method). Zeiberg and Bleich[10] have compared a finite difference calculation with results for the laminar wake from the earlier integral method solution of Bloom and Steiger.[7] Appreciable differences for the laminar wake were found between the finite difference solution and the integral solution of Reference 7. The effect of different diffusivity laws for the turbulent wake was also examined in Reference 10 and large deviations found among the results. The finite difference method is certainly the most general and a primary result of the present paper is a comparison of the present method with more elaborate numerical methods such as those of Reference 10. It should be noted that in the detailed finite difference solution, the turbulent diffusivity must be specified everywhere in the turbulent wake. It is not always straightforward to do this; even the concept of gradient diffusion is not clear at the edge of the wake.

Except for the calculation by the present authors in Reference 8 none of the nonequilibrium results obtained by the methods discussed above included a variable inviscid enthalpy field, i.e., they are all effectively "slender body" results.** However, S.C. Lin and J. Hayes[11] have compared the so-called "random inviscid convection model" with a simple one-dimensional calculation for the reacting turbulent wake of a blunt body. The random convection model ignores the fundamental nonlinear interaction

---

*Important for half-cone angles of about 20 degrees or greater.

**Recently, numerical finite-difference methods for blunt body flows, taking into account vorticity swallowing, have been developed by H. Li of the General Electric Co. and Zeiberg of GASL.

of turbulent eddies which is usually responsible for the relatively efficient mixing of a turbulent flow. Flow properties for the "turbulent wake" in their model are obtained by averaging local inviscid properties over a specified wake boundary (which is obtained from experimental evidence, or from a "homogeneous mixing model" calculation). On the other hand, the homogeneous model assumes the entrained flow adopts the local turbulent structure instantaneously. The actual physical case may well lie somewhere in between the limiting cases discussed by Lin and Hayes. However, the well-known results of Townsend[12] for incompressible wakes indicate that, for the far wake, the homogeneous mixing model is a good representation,[5] and this model is adopted here. A resolution of this question for the hypersonic wake must await detailed experimental studies.

In the Lees-Hromas model, the turbulent enthalpy-excess trail is represented by the peak (axis) enthalpy level and by the lateral extent (width) of the trail. While the velocity and stagnation enthalpy in a turbulent wake are nearly uniform after a short distance downstream,[5] a large static enthalpy excess trail persists for a hypersonic flow. For this reason, the enthalpy conservation equation is used to calculate the growth of the wake in the Lees-Hromas method. The velocity is assumed constant wherever it appears directly rather than as a difference across the wake. The essential simplicity of this model is retained herein by representing each species concentration by its axis value and by a characteristic profile width parameter. Just as for the enthalpy, the species are assumed to spread rapidly into an inhomogeneous inviscid flow with a mass diffusivity equal to the conductivity. The turbulent wake thus grows across streamlines of the inviscid flow and engulfs the species and energy contained in that flow. For blunt bodies such as meteors or for conical bodies of high cone angle, a significant part of the inviscid flow field external to the turbulent wake, but near the body, is also reacting. Therefore, the wake intercepts streamlines along which dissociation and ionization processes have occurred. On the other hand, for more slender bodies, the external flow is homogeneous with respect to species concentration, although still possessing a variable enthalphy in the radial direction. For this simpler case, only reactions in the wake itself need be considered.

To obtain the variation of the species concentrations at the axis and of the profile scale parameters with downstream distance, the species diffusion equations including chemical kinetic terms are integrated across the wake and, in addition, satisfied along the wake axis. Two first-order differential equations result for each species in the wake and these equations may be readily solved with the aid of a digital computer through a marching technique. It is also possible, by suitable simplifying assumptions, to obtain approximate but explicit solutions for several chemical processes of interest in the wake. A consideration of these solutions yields rough estimates of the relative extent of diffusion and chemical kinetic effects and suggests the range of applicability of scaling parameters.

In the chemical kinetic model studied, particular attention is given to the ion-electron reactions involved in the electron decay process. The influence of molecular and atomic oxygen attachment and associated neutralization and charge exchange reactions has been included in the study. As far as the authors are aware, previous chemical kinetic studies of wakes have not considered these attachment and charge exchange mechanisms jointly.

When complete solutions are obtained for the (laminar or turbulent) viscous-inviscid interaction problem in the base flow region and near wake,* a valid initial condition will then be available for the far wake calculation and the results of the near wake solution may then be applied directly as input to the far wake analysis. Until such time, the present analysis which treats the far wake is useful to determine the nature of coupled chemical and diffusion processes for assumed initial conditions.

---

*It should be emphasized that, while detailed numerical analyses of the laminar wake have been reported (References 9, 10 and 13), the pressure interaction between the viscous and inviscid flows was ignored in these calculations. Since it is this interaction which actually determines the solution in the near wake region (References 14 and 15), the usefulness in the near wake of analyses such as those reported in References 9, 10 and 13 is uncertain. By "near wake," the region behind the body which includes the Crocco-Lees critical point and over which the wake recompression takes place is referred to; this region may extend well beyond axis velocity ratios of the order of 0.3^{16}.

ANALYSIS*

The diffusion of species for axisymmetric (m = 1) or two-dimensional (m = 0) wake flow may be described by the boundary layer form of the species conservation equation,

$$\rho u \frac{\partial a_i}{\partial x} + \rho v \frac{\partial a_i}{\partial y} = \frac{1}{y^m} \frac{\partial}{\partial y}\left(\frac{\epsilon}{d} \rho y^m \frac{\partial a_i}{\partial y}\right) + \dot{\omega}_i d \tag{1}$$

and the overall continuity relation

$$\frac{\partial}{\partial x}(\rho u y^m) + \frac{\partial}{\partial y}(\rho v y^m) = 0 \tag{2}$$

In the above, ϵ is the local (turbulent) diffusivity, $\dot{\omega}_i$ represents local species production by reaction, and all length scales have been normalized by d. As in Reference 5, the Howarth-Dorodnitsyn transformation is used to define a new lateral scale, Y_T, for the turbulent wake

$$\rho y^m \, dy = \rho_f Y_T^m \, dY_T \tag{3}$$

where the subscript f denotes quantities at the edge of the wake.

Also, a scale for the inviscid wake is defined by

$$\rho_L y^m \, dy = \rho_\infty Y^m \, dY \tag{4}$$

The species mass fractions are assumed to be distributed as

$$\frac{a_i - a_{i_f}}{a_{i_o} - a_{i_f}} = \beta_i(x) G(\theta_i) \quad , \quad \theta_i = Y_T / Y_{s_i}(x) \tag{5}$$

so that $\beta_i(0) = 1$, $G(0) = 1$, $G(\theta_i) = 0$ for $\theta_i \geq \theta_{i_f} = Y_{T_f} / Y_{s_i}$.

---

* The notation used here is generally the same as that of Reference 5.

The constant quantities a_{i_o} are assumed known, and denote the initial species mass fractions on the axis; the variable $a_{i_f}(x)$ are either assumed known or are simultaneously calculated and denote the inviscid species at the edge of the wake. Thus, two parameters $\beta_i(x)$ and $Y_{s_i}(x)$ are used to represent the species in the wake. The first, β_i, is the relative axis mass fraction; the second, Y_{s_i}, is a characteristic mass thickness parameter. This parameter is introduced to allow the profiles to adjust their "flatness" as the diffusion proceeds. The profile $G(\theta_i)$ is assumed.* Solving Equation (2) for v, inserting into Equation (1), integrating over the wake using Equations (3) through (5), and assuming $u \approx u_f \approx u_\infty$ gives a relation for dY_{s_i}/dx which is conveniently written in terms of θ_{i_f} as

$$(m+1)\theta_{i_f}^{-1}\theta_{i_f}' = -\left[1 - (m+1)^{-1}\beta_i^{-1}P_i^{-1}\right]\left(a_{i_o} - a_{i_f}\right)^{-1} a_{i_f}'$$

$$+ (m+1)Y_f^{-1}Y_f' + \beta_i^{-1}\beta_i' - \frac{\beta_i^{-1}\, d}{\left(a_{i_o} - a_{i_f}\right)u_\infty}\frac{\phi_i}{P_i} \qquad (6)$$

where

$$P_i = \int_o^1 G\left(\theta_{i_f}\zeta\right)\zeta^m d\zeta \quad , \quad \phi_i = \int_o^1 \frac{\dot{\omega}_i}{\rho}\zeta^m\, d\zeta \quad , \quad \zeta = Y_T/Y_{T_f}$$

and the first term on the right-hand side represents the effect of reactions in the inviscid outer region.

Also, using Equations (3) through (5) in Equation (1) gives, on the axis,

---

*Studies have been made of the effect of profile shape in the present method. A comparison of calculations for the parabolic shape $G(\nu) = 1 - \nu^2$ and the cosine distribution $G(\nu) = 1/2(1 + \cos \pi\nu)$ for a given value of the diffusivity constant $KG''(0)$ indicates very close agreement in all quantities calculated, and therefore a lack of sensitivity to the specific profile chosen.

$$\beta_i' = -(1 - \beta)\left(a_{i_o} - a_{i_f}\right)^{-1} a_{i_f}'$$

$$+ (m + 1)G''(0)\beta_i \frac{\theta_{i_f}^2}{Y_{T_f}^2} \frac{\tilde{\epsilon}}{u_\infty d} + \frac{\left(a_{i_o} - a_{i_f}\right)^{-1}}{\rho(x, 0)} \frac{d}{u_\infty} \dot{\omega}_i(x, 0) \qquad (7)$$

As in the notation of Reference 5,

$$\tilde{\epsilon} = \left[\frac{\rho(x, 0)}{\rho_f}\right]^{2/(m+1)} \epsilon$$

The form used here for ϵ is identical to that assumed in References 5 [Equation (10b)] and 17 since, as discussed later, calculations using this form seem to agree well with experimental data. The effective turbulent Lewis number is thereby assumed to be unity.

Equations (6) and (7) constitute a set of relations enabling the species parameters β_i and Y_{s_i} to be calculated by integration, providing the thermal state and the width of the wake are known. These quantities may be obtained by only a slight modification of the Lees-Hromas method. This modification consists simply in replacing the approximate equation of state $p \sim \rho h$ used therein with the exact one, namely

$$p = \rho \frac{R_o}{\bar{m}} T \quad , \quad \bar{m}^{-1} = \sum_i a_i m_i^{-1}$$

With this simple modification, integration of Equations (6) and (7) may be carried out simultaneously with the integration of Equation (38) of Reference 5 for Y_f.* For the molecular specific heats, linear vibrators are

*In Reference 5 a fictitious inviscid profile between $y = 0$ and $y = y_f$ was employed. The variable Y_f was calculated for this profile and related to Y_{T_f} by introducing a quantity δ to account for the displacement effect of the turbulent wake. It has been pointed out by A. G. Hammitt that, since the variable Y is essentially a mass flux coordinate (ignoring the fact that the velocity is not quite uniform), by equating Y_f^{m+1} with $(\rho f/\rho_\infty) Y_{T_f}^{m+1}$ and carrying out the solution entirely in mass flux coordinates, the use of a fictitious profile may be avoided. The Y coordinate is then interpreted as the mass flux coordinate for the actual physical flow, rather than for a fictitious inviscid flow.

assumed, with the vibration in equilibrium. The atomic specific heats are assumed constant. These assumptions seem appropriate for the range of temperatures involved.

To obtain the inviscid species concentrations a_{i_f}, a simultaneous integration along the inviscid streamlines intersected by the turbulent wake is required. With a pressure field determined from an appropriate characteristics solution for the inviscid flow, and a given initial radial distribution, this integration becomes a straightforward procedure.

IONIZATION KINETICS

For the neutral air species in the reacting wake, the more or less standard set of reactions listed in the appendix have been employed. The rate constants used for all the reactions considered are also given there.

For the charged air species, the following set has been chosen to represent the ionization kinetics:

$$\text{G)}\quad NO^+ + e^- \rightleftharpoons N + O$$

$$\text{H)}\quad 2O_2 + e^- \rightleftharpoons O_2^- + O_2$$

$$\text{I)}\quad O + e^- + M \rightleftharpoons O^- + M$$

$$\text{J)}\quad O^- + NO^+ \rightleftharpoons NO + O$$

$$\text{K)}\quad O_2^- + NO^+ \rightleftharpoons O_2 + NO$$

$$\text{L)}\quad O + O_2^- \rightleftharpoons O^- + O_2$$

This set is of course far from complete but represents what are thought by the authors to be the most significant types of reactions involved. Reaction G) is the well-known associative ionization-dissociative recombination reaction which dominates the removal of electrons at low air density and high electron concentration.[6] Both of the attachment reactions H) and I) are considered since either may be significant mechanisms for electron removal. The electron affinity of O(~ 1.5 ev) enables earlier attachment than for O_2 which has a lower affinity (~ 0.5 ev). However, unless highly dissociated at the beginning of the wake the usually smaller atomic oxygen concentration may prohibit significant electron removal by O, especially

in the far downstream wake which is mainly molecular.[6] While the neutralization reactions J) and K) are important in the early, high temperature part of the wake, they contribute little once the temperature is reduced since the forward rates vary as the square of the charge density and the backward reactions require large activation energies. The charge exchange reaction D) may play a significant role in removing O_2^- depending on whether this reaction proceeds as a simple recombination reaction, or whether an activation energy is required.[8] This fact seems to have been overlooked in other recent analyses. The presence of positive atomic ions and radiative processes has been ignored in the ionization model; this assumption is believed to be applicable to the majority of the wake for flight speeds at or below typical re-entry vehicle velocities.

An important, yet imperfectly understood, question in chemical kinetic calculations for turbulent flows is the applicability of quasi-steady or "laminar" expressions to represent the species reaction terms $\dot{\omega}_i$.[11, 18, 19] Two (at least) crucial questions are involved, viz., the degree of homogeneity of the flow field and the use of a mean temperature to characterize the local thermal energy of the flow. As previously mentioned, the present homogeneous mixing model assumes instantaneous development of an equilibrium turbulent structure in the mass entrained by the wake. In regard to the influence of temperature fluctuations on the reaction processes, it has been suggested (e.g., Reference 18) that as long as the energy content of the fluctuations is small compared to the average static enthalpy, the molecular collision processes may remain unaffected. This criterion is certainly an upper limit; more stringent criteria are probably actually required to insure the validity of the use of quasi-steady kinetic rate expressions. However, an important point relative to turbulent nonequilibrium far wakes is that the chemical processes occurring are predominantly exothermic. Hence the dependence of the chemical rates on temperature is weak. This situation is in direct contrast to the turbulent boundary layer or perhaps near wake, both of which are usually endothermic with rates exponentially dependent on temperature. Use of quasi-steady rates for these turbulent flows thus appears more questionable than for the far wake. As pointed out in Reference 10, use of the quasi-steady assumption should be construed more as a reference to the state of the art on this subject rather than to the belief in the correctness of this assumption.

EXPLICIT SOLUTIONS FOR TURBULENT WAKE SPECIES

Since the problem has been reduced to a set of simultaneous first-order differential equations, provided p(x) is assumed, numerical solutions may be obtained with the aid of a digital computer. Examples of such solutions are given in a later section. However, it is helpful to have explicit solutions wherever possible; by the use of further simplifying assumptions, several new explicit solutions have been obtained and are discussed briefly below.

PURE DIFFUSION

Taking $\dot{\omega}_i = 0$, $a'_{i_f} = 0$ in (7) and (8) gives, on integration,

$$\theta_{i_{f_o}}^{-1}\,\theta_{i_f} = Y_{f_o}^{-1}\,Y_f\beta_i^{1/(m+1)}$$

$$\beta_i = \left[1 + 2G''(0)\frac{\theta_{i_{f_o}}^2}{Y_{f_o}^2}\int_{x_o}\frac{\tilde{\epsilon}}{u_\infty d}\left(\frac{\rho_f}{\rho_\infty}\right)^{2/(m+1)}dx\right]^{-(m+1)/2} \tag{8}$$

To obtain further simplification, it is assumed that the entire inviscid drag is contained within the wake; then the wake growth obeys a simple power law. For example,[20] for an axisymmetric body (m = 1),

$$Y_f/Y_{f_o} = X^{1/3}$$

$$2G''(0)\frac{\tilde{\epsilon}}{u_\infty d}Y_f^{-2} = \frac{2}{3}\Lambda X^{-1} \tag{9}$$

$$T/T_\infty = 1 + \Lambda_1 X^{-2/3}$$

wherein

$$\Lambda = -\frac{3}{16}\frac{G''(0)}{G_1} K C_D / Y_{f_o}^3 \cdot \Lambda_1 = \frac{(\gamma_\infty - 1)}{16 G_1} M_\infty^2 \frac{C_D}{Y_{f_o}^2}$$

and

$$\chi = 1 + \Lambda(x - x_o)$$

Inserting the above into (8) gives

$$\beta_i^{-1} = 1 + \theta_{i_{f_o}}^2 (\chi^{2/3} - 1)$$

$$\theta_{i_f} = \theta_{i_{f_o}} \chi^{1/3} \beta_i^{1/2}$$

Thus, at small x for $\theta_{i_{f_o}} < 1$ the particle density on the wake axis n_i, increases and the characteristic species scale, Y_{s_i}, decreases. The converse is true for $\theta_{i_{f_o}} > 1$. At large distance,

$$n_i / n_{i_o} \approx \frac{\Lambda_1}{\theta_{i_{f_o}}^2} (\Lambda x)^{-2/3}, \qquad \theta_{i_f} \approx 1$$

Further, at all distances when $\theta_{i_{f_o}} = 1$,

$$n_i / n_{i_o} = \left(1 + \Lambda_1^{-1} \chi^{2/3}\right)^{-1}, \qquad \theta_{i_f} = 1$$

The physical explanation of these simple results is clear. Since the diffusion is turbulent with equal mass and energy diffusivities (Le = 1), the species concentrations in the absence of reactions diffuse exactly as the enthalpy does. The species have the overall constraint of constant total particle number over the wake; the enthalpy has the constraint of constant drag within the wake. Thus, if the initial density distribution is "flatter" than the enthalpy distribution (i.e., if $\theta_{i_{f_o}} < 1$), the species distribution will tend to become "sharper" as the wake growth commences and the axis concentration will increase. The converse is true for an initially "sharper" species distribution. In the limit of large distance,

the species and enthalpy distribution become identical ($\theta_{i_f} = 1$) and the axis concentration obeys the well-known 2/3 power law. The chemical production of species in the wake will certainly modify this process. While electron decay processes in the wake are generally rapid relative to diffusion, the recombination of atoms is generally slow. Consequently, the pure diffusion case studied above may be a valid approximation for the atomic species but is significantly modified by chemical kinetic effects for the electron density.

ATOM RECOMBINATION WITH COUPLED DIFFUSION

Further simple solutions may be obtained if only one species parameter is considered. Taking $\theta_{i_f} = 1$ in either (6) or (7) will yield an immediate solution if $\dot{\omega}_i$ is sufficiently simple. For example, for the recombination of atoms,

$$\dot{\omega}_A = -4k_{r_A} \frac{\rho^3}{\mathcal{M}^2} a_A^2 \tag{10}$$

wherein a factor $1 + a_A$ has been replaced by unity since $a_A << 1$. Inserting (10) into (7) with $\theta_{i_f} = 1$ gives, on integration

$$a_A^{-1} = f_A(x) \left[a_{A_o}^{-1} + \int_{x_o} A_1(x) f_A^{-1}(x) dx \right] \tag{11}$$

where

$$A(x) = \frac{2G''(0)}{Y T_f^2} \frac{\tilde{\epsilon}}{u_\infty d}, \quad A_1(x) = \frac{4}{\mathcal{M}^2} \frac{\rho_\infty^2 d}{u_\infty} \frac{\rho^2(0,x)}{\rho_\infty^2} k_{r_A}, \quad f_A(x) = \exp\left[- \int A(x) dx \right]$$

To simplify further, a specific reaction rate $k_{r_A} = a_{r_A} T^{-3/2}$ is assumed and the relations (9) are applied. Then with $\rho \sim T^{-1}$

$$a_A^{-1} = \chi^{2/3} \left[a_{A_o}^{-1} + \frac{3}{2} \frac{\lambda_A}{\Lambda} \int_1^{\chi^{2/3}} \nu^3 \left(\Lambda_1 + \nu \right)^{-7/2} d\nu \right]$$

where

$$\lambda_A = \frac{4 a_{r_A}}{T_\infty^{3/2} \mathcal{M}^2} \frac{\rho_\infty^2 d}{u_\infty}$$

The integral is readily evaluated; for $x \gg \Lambda^{-1}$

$$a_A^{-1} \approx (\Lambda x)^{2/3}\left[a_{A_o} + \frac{3\lambda_A}{\Lambda}(\Lambda x)^{1/3}\right] \tag{12}$$

Thus, the atom concentration diffuses as $x^{-2/3}$ and recombines as x^{-1}. The recombination will exceed the diffusion for distances greater than

$$x_{D_A} = \Lambda^2\left(3a_{A_o}\lambda_A\right)^{-3}$$

With $a_{r_A} \approx 10^{19}$ and since $\Lambda^2 \approx 10^{-3}\, C_D^{-1} T/T_f$, then for a typical value

$$a_{A_o}^{-3}\, C_D^{-1} T_\infty/T_f = 10^2$$

and with $U_\infty/d = 10^4$ sec^{-1}, there results $x_{D_A} \approx 10^{-30}\rho_\infty$ (ρ_∞ in gm/cc). Thus, at about 100 kft altitude and below, recombination becomes the dominant process for the decay of the axis atom concentration and a linear decay with distance is predicted. Above this altitude, the atom concentration is dominated by diffusion.

ELECTRON RECOMBINATION, ATTACHMENT, AND DIFFUSION

A solution for the electron decay process may be obtained in the same fashion. Considering only electron recombination and attachment to molecular oxygen

$$\frac{\dot{\omega}_e}{\mathfrak{M}_e} = -k_{r_e} n_e^2 - k_a n_{o_2}^2 n_e$$

and inserting into (7) gives, upon integration

$$n_e^{-1} = \frac{\rho_o}{\rho(x,o)} f_e(x)\left[n_{e_o}^{-1} + \int_{x_o} A_2(x) f_e^{-1}(x)dx\right]$$

where

$$A_2(x) = \frac{d}{u_\infty} k_{r_e} \frac{\rho(x,0)}{\rho_o}, \quad A_3(x) = \frac{d}{u_\infty} k_a n_{o_2}^2 \text{ and } f_e(x) = \exp\left[- \int_{x_o} (A - A_3) dx \right]$$

This result is directly analogous to that which Lees[6] originally obtained by applying an integral equation across the wake rather than along the wake axis. With the wake growth given by (9), and taking

$$k_{r_e} = a_{r_e} T^{-3/2}, \quad k_a = \text{const}, \quad \rho \sim T^{-1}$$

then

$$n_e^{-1} = \frac{1 + \Lambda_1 \chi^{-2/3}}{1 + \Lambda_1} f_e(x) \left[n_{e_o}^{-1} + \frac{3}{2} \frac{\lambda_{e_r}}{\Lambda} \int_1^{\chi^{2/3}} \frac{f_e^{-1}(\nu^{3/2}) \nu^3}{(\Lambda_1 + \nu)^{5/2}} d\nu \right]$$

where

$$f_e(\chi) = \chi^{2/3} \exp\left[\frac{3}{2} \frac{\lambda a}{\Lambda} \int_1^{\chi^{2/3}} \frac{\nu^{5/2}}{(\Lambda_1 + \nu)^2} d\nu \right]$$

and

$$\lambda_{e_r} = \frac{a_{r_e}}{T^{3/2}} (1 + \Lambda_1) \frac{d}{u_\infty}, \quad \lambda_a = k_a \frac{a_{o_2}^2}{m^2} \frac{\rho_\infty^2 d}{u_\infty}$$

For

$$\lambda_a >> x >> \Lambda^{-1}$$

i.e., at large x but with negligible attachment,

$$n_e^{-1} = \Lambda_1^{-1} (\Lambda x)^{2/3} \left[n_{e_o}^{-1} + \frac{3\lambda_{e_r}}{n_{e_o}} (\Lambda x)^{1/3} \right] \tag{13}$$

a result similar to (12) for atom recombination. Here, electron recombination prevails over diffusion beyond $x_{D_e} = \Lambda^2 (3 n_{e_o} \lambda_{e_r})^{-3}$. Taking $a_{r_e} \approx 2 \times 10^{21}$, then for typical values of $u_\infty/d = 10^4$ sec^{-1}, $C_D^{-1} T_\infty / T_f \approx 10$ there results $x_D \approx 10^{24} n_{e_o}^{-3}$ and it is necessary for the initial electron level, n_{e_o}, to be lower than 10^8 cm^{-3} for diffusion to play a significant role in the electron level decay. However, for a small blunt body with $u_\infty/d = 10^6$ sec^{-1}, $T_o/T_\infty = 20$, $C_D^{-1} T_\infty / T_f = 10^{-1}$ then $x_{De} \approx 10^{35} n_{e_o}^{-3}$

and diffusion dominates much of the wake for initial electron densities as high as 10^{11} cm^{-3}. The strong dependence on the initial electron level and temperature ratio is clear. These quantities increase rapidly with flight speed so that the electron decay behavior in the diffusion-recombination region for small bodies should show large variations as the flight speed is increased. When $x \gg\gg \lambda_a^{-1}$ then

$$n_e \approx n_{e_o} \Lambda_1 (\Lambda x)^{-2/3} \exp(-\lambda_a x)$$

and the decay is exponential. With $k_a = 10^{18}$, $\lambda_a = 4 \times 10^{13} \rho_\infty d/u_\infty$ and for $u_\infty/d \approx 10^4$ sec^{-1} then $\lambda_a \approx 4 \times 10^9 \rho_\infty^2$. Therefore, at 100 kft, attachment is significant beyond distances of the order of $x \approx 10$ whereas at 150 kft a distance of the order of $x \approx 10^3$ is required. However, at $x \approx 10$ behind the body the wake temperature is still relatively high and the detachment reaction (which has been ignored) will prevent a significant accumulation of O_2^- ions; that is, below 150 kft the attachment-detachment reaction is nearly in equilibrium. When the wake temperature finally falls below some critical level, attachment will then rapidly absorb the remaining electron concentration, leaving only O_2^- and NO^+ in the wake. Thus, for a fully turbulent wake, since the distance x necessary for the wake temperature to fall below the critical attachment temperature is essentially independent of altitude, the final electron "clean-up" in the wake due to attachment will occur at about the same x for all altitudes below about 150 kft until the recombination reaction goes into equilibrium.

NUMERICAL RESULTS*

Detailed numerical calculations are given herein for a variety of body shapes and sizes: a large slender cone, a small 6 degree cone with several blunt nose shapes, a large 12 degree sphere cone, and a small sphere. The comparison of present results with those of other analyses is made for the large slender cone. The blunt body shape study is carried out for the small 6 degree cone with three nose shapes. Wakes with contaminants are calculated for a large blunt body and a large slender body. The calculations of the wakes of a small sphere are for comparison with ballistic range results.

For slender body cases, the inviscid enthalpy and pressure distributions, which are required as an input to the wake solutions, were obtained from an equilibrium characteristics program as discussed in References 5 and 20. For blunt bodies, an equilibrium characteristics solution was used to generate pressure distributions, then nonequilibrium streamtube calculations were carried out to determine the rest of the inviscid flow field variables. In Figure 1, inviscid enthalpy distributions, normalized by the axis value $h_L(o)/h_\infty - 1 \equiv H$, are shown for several of the cases considered. The slender cone distribution is, of course, flat out to the point where the expansion from the cone shoulder intersects the bow shock. The enthalpy then rapidly diminishes to the ambient level at larger streamline distances. Due to nonequilibrum effects, the blunt cone enthalpy varies in the nose region, as shown in Figure 1. Twelve inviscid streamtubes were calculated in order to define the shape of the profile shown. The nose and base diameters for the 47-6 degree bi-conic shape considered were 2.4 and 9 inches respectively; the base diameter is used to normalize the radial coordinate. Wake pressure distributions as suggested in References 5 and 20 were employed in the calculations; however, the influence of the assumed variation of pressure in the wake is actually confined to a very short distance downstream.

---

*The computer program was written for an IBM 7094 by Maureen L. Sprankle. A standard Adams-Moulton-Runge Kutta (AMRK) predictor-corrector routine was used for some cases given. For others a method recently suggested by Treanor[21] was applied; the latter appears to improve calculation time significantly in near equilibrium cases. An attempt to improve upon the Treanor method for a coupled set of species is currently being pursued.

SLENDER CONE—COMPARISON WITH OTHER METHODS*

For sufficiently slender bodies, temperatures in the inviscid flow are inadequate for the generation of appreciable ionization or dissociation phenomena; thus, the inviscid flow is nonreacting. A typical case of this kind has been considered, an 8 degree cone of 2.82 feet diameter at U_∞ = 22 kft/sec and 150 kft altitude. Recent experimental data indicate that the flow near the wake neck of such a slender body may be stable over a large range of Reynolds number and that the transition location moves toward the neck with increasing Reynolds number.[13, 23, 24, 25] A length of "laminar run" may therefore precede the turbulent wake, providing the Reynolds number is not so large that the body flow or free-shear layer flow before the neck is turbulent. The exact conditions under which the upstream flow becomes turbulent depend on details such as angle of attack, ablation effects, wall temperature and roughness, and are difficult to precisely predict. However, a transition location was estimated using the laboratory data correlation of Reference 13.

Species concentrations for the laminar run were calculated along the axis and several other streamlines by using a one-dimensional reacting streamline model. The initial composition of the gas at the start of the laminar run as well as the stagnation enthalpy and velocity history for the laminar streamlines were taken from estimates for these quantities made by A. Pallone.* The initial enthalpy ratio used, $h(0)/H_\infty = 0.30$ is of the order indicated by applying to the near wake the approximate model of Chapman[26] as modified by Denison and Baum.[27] As shown in Figure 2, a comparison of electron density obtained by the detailed laminar calculations of Zeiberg, Lien, and Li indicates that the chemical processes

*Results from the present theory are compared here with results obtained by the methods given in References 9 and 10 and with unpublished calculations of H. Li of The General Electric Co. The last two are finite difference calculations. The method of Reference 9 is a "strip" method for laminar flow and an integral method for turbulent flow (previously discussed). By agreement, the same initial conditions for the laminar run were assumed for each method. However, each group performing the calculations made its own estimate of the location of transition. The authors wish to thank A. Pallone, AVCO; W. Daskin, GASL; and H. Lew, GE for making these calculations available. They were initially reported in part in Reference 22.

determined by the present simple method closely reproduce results obtained by these detailed calculations. Thus, the principal effect of the short laminar run is to allow time for chemical reactions to proceed and near equilibrium species concentrations result. At the estimated location of the transition point, the "laminar" streamline properties there were used to determine levels and distributions for the turbulent wake calculation; the axis velocity ratio at this point was $u/u_\infty = 0.6$, hence several diameters would actually be required for the rapid turbulent diffusion to raise this ratio to the assumed value of near unity (see section on Comparison with Experiment). The resulting axis charged particle concentrations calculated for the turbulent wake are also given in Figure 2. The attachment of electrons to atomic oxygen is seen to begin before an x/d of about 10^2 and later to molecular oxygen just beyond this distance where the temperature is low enough (below about 800°K) to permit stable O_2^- ions. The familiar linear recombination decay with distance predominates at smaller distances, except for an even sharper drop in electron concentration immediately after transition. This drop is particularly noticeable in the present calculations and those of Zeiberg. It is due to the fact that the effective thickness of the electron distribution is initially smaller than the enthalpy thickness at the transition point; beyond this point the electrons then rapidly diffuse outward to the edge of the wake and the axis concentration is lowered. The agreement between the various theoretical methods is reasonably good over the entire range of the calculation.

The temperature calculated for the axis of the wake is shown in Figure 3. Although the temperature decrease shown for the turbulent wake is quite rapid in comparison with the laminar result, nevertheless, temperature levels as high as 1000°K still exist at 100 body diameters downstream. Beyond 500 diameters, the wake intercepts the inviscid streamline from the expansion-shockwave intersection point and a slightly more rapid temperature decrease then results as the wake mixes with the colder inviscid fluid. The divergence among the various theoretical methods appears

to be mainly due to the fact that somewhat different estimates were made for the location of transition in each calculation.* Thus, accidentally, these results indicate the effect of transition location on the axis temperature history.

Axis mass fractions for N, O, and NO are shown in Figure 4 for the present calculations. The N concentration rapidly diminishes in the turbulent wake due to the rapid NO "shuffle" reactions as the temperature is lowered. However, the O concentration disappears mainly by simple diffusion, as previously suggested by the order of magnitude estimates of the extent of the diffusion controlled versus recombination controlled wake given by the explicit solutions.

In Figure 5 mean electron density contours are shown. Note that the electron attachment to molecular oxygen near the low temperature edge of the wake results in an electron distribution width significantly smaller than the wake width. This effect is necessarily confined to the low electron level region of the wake. A simple one-parameter integral method does not allow the calculation of such effects; however they are reasonably represented in the present method.

BLUNT-NOSED CONE

Three different blunt cone shapes were considered as shown in Figure 8: a sphere cone, a "flat" faced cone and a 47 degree -6 degree biconic shape. The nose radii were taken so that the estimated overall drag coefficients were the same. The inviscid blunt cone flow fields contain dissociated and ionized species up to the radial stream coordinate where the shoulder expansion reduces the shock strength. The production of these species is cut off at the shoulder by the expansion and the partially ionized and dissociated gas there (which is nearly frozen due to the low pressure and high velocity) then forms the inviscid wake. For example, in Figure 6 the radial distributions of a_O, a_N, a_{NO} and temperature in the

*Comparisons of the theoretical methods were also carried out at 100 kft altitude for a completely turbulent wake (Reference 22). In these calculations, the temperature levels, as well as electron levels, agreed quite well among the various methods.

inviscid flow field at the start of the wake calculations for the 47 degree -6 degree biconic shape are shown;* these values occurred at the point where p/p = 4. With this distribution as a starting condition, along with the values of the other species in the inviscid flow, the behavior of the turbulent wake growing into the dissociated, ionized, and reacting inviscid field of this blunt body was calculated. Although not shown, the inviscid flow fields for the other two blunt shapes were similarly determined and used as initial conditions for the turbulent wake calculation of these bodies.

Shown in Figure 7 are the resulting turbulent axis and wake edge temperature for the biconic configuration; an initial axis value $h(0)/H_s = 0.6$ was assumed. Figure 8 shows the axis and edge electron concentrations for all three blunt nose shapes studied. The axis values in the turbulent wake were assumed to be in equilibrium at the initial station. The effect of the reacting inviscid flow in maintaining a high electron concentration, until the shoulder expansion fan-shockwave intersection streamline is reached, is apparent. The irregular behavior of the edge temperature as shown in Figure 7 results from chemical kinetic effects at the shockwave-shoulder expansion intersection region and is also apparent in Figure 8. Each shape considered had the same inviscid drag coefficient. However, the momentum defect is spread out to a larger radial distance by the conical nose shape hence high electron concentrations are maintained farther downstream for this shape.[20] At lower altitudes, where the core drag is initially a smaller fraction of the overall drag, the cone wakes are even longer in comparison with the other bodies.

CONTAMINATED WAKES

The almost universal presence of trace amounts of low ionization potential substances such as sodium in the materials ablating from high speed bodies ensure the generation of high electron concentrations in the flow field even at low ambient pressure. Since this ablating material may well cause a significant extension of the electron trail length, it is of interest

*The large gradients in the supposed inviscid flow at the shoulder expansion-shock intersection will certainly cause a smearing out of these profiles by molecular diffusion in the actual physical case. However, over lengths of interest this effect is probably small.

to estimate the effect of the contaminant on the electron density history in the wake. For this purpose, the following reactions have been added to the chemical kinetic set:

$$Na^+ + e^- + X \rightleftharpoons Na + X$$

$$Na + O + O \rightleftharpoons O_2 + Na^+ + e^-$$

$$Na^+ + O^- \rightleftharpoons O_2 + Na^+ + e^-$$

$$Na^+ + O^- \rightleftharpoons Na + O$$

$$Na^+ + O^- \rightleftharpoons Na + O_2$$

$$Na + NO^+ \rightleftharpoons Na^+ + NO$$

Some of the chemical rates for the above reactions have been measured, others only estimated. The values used here were taken from the recent survey report by Bortner;[28] based on these values, the above reactions are believed to be the most important.

Calculations were carried out for the contaminated wakes of a slender and a blunt body and compared with pure air results for the same cases. As before, Le = 1 has been assumed for all species in the turbulent wake. Bortner[28] and others[29, 30] have found that primarily due to the Na + O neutralization reaction above, followed by the collisional detachment of the electron from O^-, the sodium will produce equilibrium ionization levels both in the boundary layer and laminar run at 150 kft altitude. Thus, the level of electrons obtained depends only on the level of contaminants present in the heat shield. Typical values which have been measured[29] are 10 to 100 parts/million. For the present calculations, initial mass fractions in the wake of 10^{-5} and 10^{-6} (heat shield level diluted by a factor of 10) were assumed for the sodium and the sodium was assumed to be 90 percent ionized. Results are shown in Figure 9A for a blunt body and Figure 9B for a slender body. It is interesting to note that the initial levels of electrons are not altered much for any of the cases calculated; however, the

downstream decay is altered significantly for both the blunt and slender bodies. This is due to the slow recombination of the "sodium electrons" until temperatures low enough for oxygen attachment are achieved.

COMPARISON WITH EXPERIMENT

Wake Velocity

Wake widths calculated by the original Lees-Hromas equilibrium theory[5] have shown excellent agreement with the early (low Mach number) ballistic range data for the small spheres of Slattery and Clay.[25] More recently, Knystautas[31] at CARDE has confirmed this agreement for sphere sizes as large as 3 inches. Strong support is therefore given to the diffusivity model proposed in References 5 and 17. While measurements of details of hypersonic wakes other than wake width are still scarce, some data on wake velocity are available. Primich[32] has obtained microwave Doppler-shift measurements of the wake velocity of small spheres and Washburn, Goldburg and Melcher[33] have reported measurements of wake velocity using the luminous streak method. While in both cases the interpretation of the data obtained is not entirely straightforward, it is of interest to compare wake velocities calculated by the present theoretical model with the experimentally observed results. In Figure 10, wake velocities relative to a coordinate system fixed in the laboratory are plotted versus axial distance for the sphere and cone data referred to. The theoretical curves represent calculated wake axis velocities; these calculations were carried out for conditions representative of the range over which the data were taken. The cone data were taken directly from Figure 2 of Reference 33; a comparison of a curve fit of these data with the theory (as well as with that of Reference 9) has already been given in Reference 33. The data are included here merely for reference purposes. The sphere data of Primich shows a much slower decay than for cones with again a reasonable agreement with theory. It is significant that although the present theory does not calculate the initial low velocity region correctly, this discrepancy is limited to the first 5 to 15 diameters; thereafter a close agreement with experiment is obtained.

Electron Density

The large variation in inviscid enthalpy results in chemical relaxation processes over a significant portion of the flow behind a sphere. Calculations of this inviscid wake by S.C. Lin and J. Hayes[11] indicate that, for large bodies, the wake may intercept ionized and dissociated species in the inviscid stream as far back as 100 diameters behind the body. However, for small bodies the relatively larger skin friction drag causes the wake width to begin at a larger value; farther downstream the outer inviscid flow is essentially molecular in composition and only kinetics in the turbulent wake need be considered. Calculations for several ballistic firing range conditions are shown in Figures 11A and 11B. The data shown were obtained at the Lincoln Laboratory, MIT, using a resonant cavity technique which yields linear electron density.* Although early data[34] evidenced large variations from run to run, apparently due to range contaminants, the experimental difficulties appear to have been overcome and consistent repeatable data are now available.

Experimental results at 80 mm pressure were first chosen to compare with calculations from the present theoretical model. An enthalpy ratio at x = 0 of $h(0)/H_s = 0.5$ was taken and, due to the high temperature associated with this enthalpy level, the initial species concentrations at x = 0 were taken to be in equilibrium at the local temperature and pressure ($4\ p_\infty$). The results of the calculation are shown in Figure 11A. At 80 mm pressure available experimental data indicates that transition of the wake should occur within about 20 diameters, hence an entirely turbulent wake was assumed in the calculation. In this case, fair agreement (within a factor of two) with the measured electron level was obtained, except beyond 5000 diameters where the experimental results indicate a faster electron decay at lower electron levels than predicted.

A calculation for 40 mm ambient pressure is shown in Figure 11B. For this case, an estimate of the nonequilibrium laminar run (similar to that described above for the slender cone case) was carried out to the

*The authors are indebted to R. Slattery and W. Kornegay of the Lincoln Laboratory, MIT, for providing this recent unpublished data.

x/d = 150 station, which was the estimated transition location. The present method was then applied to the prediction of the electron line density in the far wake. As indicated in Figure 11B, the procedure described above appears to overestimate the electron level from 10^2 to 10^3 diameters and underestimates it from 10^3 to 10^4 diameters. The disagreement prior to 10^3 is attributable to the necessarily approximate treatment of the laminar wake and the uncertainty in initial conditions. Beyond 10^3 diameters, the electron density history is mainly sensitive to the chemical rates which have been estimated for the clean-up reactions. Specifically, since oxygen attachment dominates the electron removal beyond 10^3 diameters, the rates taken for the attachment processes apparently need further study.

While the agreement of the electron density calculations with experimental measurements is encouraging, a final decision on the accuracy of the theoretical model must await the accumulation and evaluation of more data over a wider range of experimental conditions than is currently available. Measurements of volume density in the wake concurrent with line density results, further independent chemical kinetic measurements of the pertinent reactions discussed herein over a range of temperatures, and additional information on transition and on the distance required for the establishment of a developed turbulent structure, would assist in the evaluation of the theory.

ACKNOWLEDGEMENT

The authors gratefully acknowledge their stimulating discussions with Prof. Lester Lees of the California Institute of Technology and Dr. A.G. Hammitt of Space Technology Laboratories.

REFERENCES

1. P.W. Millman, "An Observational Survey of Meteor Trails," ARS 17th Annual Meeting, Paper No. 2659-62, November 1962.

2. M.H. Bloom and M.H. Steiger, "Hypersonic Axisymmetric Wakes Including Effects of Rate Chemistry," TR 180, General Applied Science Labs, August 1960.

3. L. Ting and P. Libby, "Fluid Mechanics of Axisymmetric Wakes Behind Bodies in Hypersonic Flow," TR 145A, General Applied Science Labs, June 1960.

4. P. Lykoudis, "The Growth of the Hypersonic Turbulent Wake Behind Blunt and Slender Bodies," RM-3270-PR, Rand Corporation, January 1963.

5. L. Lees and L. Hromas, "Turbulent Diffusion in the Wake of a Blunt Nosed Body at Hypersonic Speeds," 6110-0004-MU-000, Space Technology Laboratories, Inc., July 1961. Also J.A.S., vol. 29, No. 8, p. 976, 1962.

6. L. Lees, "Hypersonic Wakes and Trails," ARS 17th Annual Meeting, Paper No. 2662-62, November 1962. Also AIAA Journal, vol. 2, No. 3, p. 417, 1964.

7. M.H. Bloom and M.H. Steiger, "Diffusion and Chemical Relaxation in Free Mixing," IAS 31st Annual Meeting, Paper No. 63-67, January 1963.

8. W.H. Webb and L. Hromas, "Turbulent Diffusion of a Reacting Gas in the Wake of a Sharp Nosed Body at Hypersonic Speeds, 6130-6362-RU-000, Space Technology Laboratories, Inc., April 1963.

9. H. Lien, I. Erdos, and A. Pallone, "Non-equilibrium Wakes with Laminar and Turbulent Transport," AIAA Conference on Physics of Entry into Planetary Atmospheres, Paper No. 63-447, August 1963.

10. S. Zeiberg and G. Bleich, "Finite Difference Calculation of Hypersonic Wakes," AIAA Conference on Physics of Entry into Planetary Atmospheres, Paper No. 63-448, August 1963. Also AIAA Journal.

11. S.C. Lin and J.E. Hayes, "A Quasi-One-Dimensional Model for Chemically Reacting Turbulent Wake of Hypersonic Objects," AIAA Conference on Physics of Entry into Planetary Atmospheres, Paper No. 63-449, August 1963.

12. A.A. Townsend, The Structure of Turbulent Shear Flow, Cambridge University Press, Cambridge, England, ch. 7, 1956.

13. A. Pallone, J. Erdos, and J. Eckerman, "Hypersonic Laminar Wakes and Transition Studies," AIAA Journal, vol. 2, No. 5, p. 855, 1964.

14. L. Crocco and L. Lees, "A Mixing Theory for the Interaction Between Dissipative Flows and Nearly Isentropic Streams," J. A. S., vol. 19, No. 10, p. 649, October 1952.

15. L. Lees and B. Reeves, "Supersonic Separated and Reattaching Laminar Flows 1. General Theory and Application to Adiabatic Boundary Layer - Shock Wave Interactions," GALCIT Separated Flows Research Project Report No. 3, October 1963.

16. W.H. Webb, R.J. Golik, and L. Lees, "Preliminary Study of the Viscous-Inviscid Interaction in the Laminar Supersonic Near Wake," 6453-6004-KU-000, TRW Space Technology Laboratories, July 1964.

17. L. Ting and P. Libby, "Remarks on the Eddy Viscosity in Compressible Mixing Flows," IAS Journal, vol. 27, No. 10, pp. 797-798, October 1960.

18. A. Ferri, P.A. Libby, and V. Zakkay, "Theoretical and Experimental Investigation of Supersonic Combustion," PIBAL Report 713, September 1962.

19. S. Corrsin, "Statistical Behavior of a Reacting Mixture in Isentropic Turbulence," Phy Fluids, vol. 1, No. 1, pp. 42-47, January-February 1958.

20. L. Hromas and L. Lees, "Effect of Nose Bluntness on the Turbulent Hypersonic Wake," 6130-6259-KU-000, Space Technology Laboratories, Inc., October 1962.

21. C.E. Treanor, "A Method for Numerical Integration of Coupled First Order Differential Equations with Greatly Different Time Constants," CAL Report AG-1729-A-4, January 1964.

22. H. Lien, A. Pallone, and J. Erdos, "Comparison and Discussion on Wake Flow Field Calculations," TM 64-40, AVCO/RAD, July 1964 (prepared for 17th AMRAC Meeting).

23. W. H. Webb, L. Hromas, and L. Lees, "Hypersonic Wake Transition," AIAA Journal, 1, 3, p. 720, 1963.

24. A. Demetriades, "Hot-Wire Measurements in the Hypersonic Wakes of Slender Bodies," AIAA Journal, vol. 2, No. 2, p. 243, February 1964.

25. R.E. Slattery and W.G. Clay, "The Turbulent Wake of Hypersonic Bodies," ARS Preprint 2673-62, November 1962.

26. D.R. Chapman, D.M. Kuehn, and H.K. Larson, "Investigation of Separated Flows in Supersonic and Subsonic Streams with Emphasis on the Effect of Transition," NACA Report 1356, 1958 (supersedes NACA TN 3869).

27. M. Denison and E. Baum, "Compressible Free Shear Layer with Finite Initial Thickness," AIAA Journal, vol. 1, No. 2, p. 342, 1963.

28. M.H. Bortner, "The Chemical Kinetics of Sodium in Re-entry," Report No. 64SD810, General Electric Corp., June 1964.

29. S. Howard, "Application of an Approximate Boundary Layer Analysis to Nonequilibrium Trace Species," to be published.

30. M. Leonard, "Ionization of Cesium and Sodium Contaminated Air in the Hypersonic Slender Body Boundary Layer, Report No. R64SD22, General Electric Corp., August 1964.

31. R. Knystautas, "The Growth of the Turbulent Inner Wake Behind a 3 Inch Diameter Sphere," T.R. 488/64, Canadian Armament Research and Development Establishment, February 1964.

32. R. Primich and M. Steinberg, "A Broad Survey of Free-Flight Range Measurements from the Flow About Spheres and Cones," TR 63-224, General Motors Corp., Defense Research Labs, September 1963.

33. W.K. Washburn, A. Goldburg, and B.W. Melcher, "Hypersonic Cone Wake Velocities Obtained from Streak Pictures," AIAA Journal, vol. 2, No. 8, p. 1465, August 1964.

34. M. Labitt, "The Measurement of Electron Density in the Wake of a Hypervelocity Pellet Over a Six-Magnitude Range, TR No. 307, Lincoln Laboratory, MIT, April 1963.

35. J.G. Hall, A. Eschenroder, and P. Marrone, "Blunt-Nose Inviscid Air Flows with Coupled Non-equilibrium Processes," J.A.S., vol. 29, No. 9, p. 1038, 1962.

36. P. Nawrocki, "Reaction Rates," 61-2-A, Geophysics Corporation of America, 1961.

37. S.C. Lin and J.D. Teare, "Rate of Ionization Behind Shock Waves in Air," AVCO/Everett Research Report 115, 1962.

38. L. Chanin, A. Phelps, and A. Biondi, "Measurements of the Attachment of Low-Energy Electrons to Oxygen Molecules," Phys Rev, vol.128, No. 1, p. 219, 1962.

APPENDIX

Species Identification Numbers

1) N_2
2) O_2
3) NO
4) N
5) O
6) NO^+
7) e^-
8) O^-
9) O_2^-

Neutral Species Reactions

A) $N + N + M \rightleftharpoons N_2 + M$

B) $O + O + M \rightleftharpoons O_2 + M$

C) $N + O + M \rightleftharpoons NO + M$

D) $N + O_2 \rightleftharpoons NO + O$

E) $NO + N \rightleftharpoons N_2 + O$

F) $2NO \rightleftharpoons N_2 + O_2$

Charged Species Reactions

G) $NO^+ + e^- \rightleftharpoons N + O$

H) $O_2 + e^- + M \rightleftharpoons O_2^- + M$

I) $O + e^- + M \rightleftharpoons O^- + M$

J) $O^- + NO^+ \rightleftharpoons O + NO$

K) $O_2^- + NO^+ \rightleftharpoons NO + O_2$

L) $O_2^- + O \rightleftharpoons O^- + O_2$

Reaction Rate Table

Catalyst, M	Reaction	a_f	b_f	n_f	a_b	b_b	n_b
1	A	0.276E17	0	-0.5	0.502E18	0.113E6	-0.5
2	|	0.109E17	|	-0.5	0.198E18	|	-0.5
3	|	0.109E17	|	-0.5	0.198E18	|	-0.5
4	|	0.236E22	|	-1.5	0.429E23	|	-1.5
5	A	0.109E17	0	-0.5	0.198E18	0.113E6	-0.5
1	B	0.617E16	0	-0.5	0.103E18	0.594E5	-0.5
2	|	0.799E20	|	-1.5	0.133E22	|	-1.5
3	|	0.301E16	|	-0.5	0.502E17	|	-0.5
4	|	0.301E16	|	-0.5	0.502E17	|	-0.5
5	B	0.225E21	0	-1.5	0.375E22	0.594E5	-1.5
1	C	0.102E21	0	-1.5	0.408E21	0.755E5	-1.5
2	|	0.102E21	|	|	0.408E21	|	|
3	|	0.200E22	|	|	0.800E22	|	|
4	|	0.102E21	|	|	0.408E21	|	|
5	C	0.102E21	0	-1.5	0.408E21	0.755E5	-1.5
-	D	0.133E11	0.356E4	1.0	0.319E10	0.197E5	1.0
-	E	0.163E14	0	0	0.741E14	0.378E5	0
-	F	0.241E24	0.430E5	-2.5	0.456E25	0.646E5	-2.5
-	G	0.181E22	0	-1.5	0.302E14	0.325E5	-0.5
1	H	0.100E17	0	0	0.600E8	0.533E4	1.5
2	|	0.100E19	|	|	0.600E10	|	|
3	|	0.100E17	|	|	0.600E8	|	|
4	|	0.100E17	|	|	0.600E8	|	|
5	H	0.100E17	0	0	0.600E8	0.533E4	1.5
1	I	0.110E20	0	-1.0	0.112E12	0.162E5	0.5
2	|	|	|	|	|	|	|
3	|	|	|	|	|	|	|
4	|	|	|	|	|	|	|
5	I	0.110E20	0	-1.0	0.112E12	0.162E5	0.5
-	J	0.100E19	0	-0.5	0.653E19	0.918E5	-1.0
-	K	0.100E19	0	-0.5	0.111E20	0.103E6	-1.0
-	L	0.122E13	0.533E4	0.5	0.208E13	0.162E5	0.5

Reaction Rate Constants:

$$\text{Forward Rate: } k_f = a_f T^{n_f} \exp\left(-b_f/T\right)$$

$$\text{Backward Rate: } k_b = a_b T^{n_b} \exp\left(-b_b/T\right)$$

Units: $(cm^3/gm\ mole)^n\ sec^{-1}$, where n is reaction order, and temperature must be expressed in degrees Kelvin.

The numerical exponent symbol, E, is standard Fortran notation; e.g., 0.1E10 means 0.1×10^{10}.

Sources for rates: References 35 through 38.

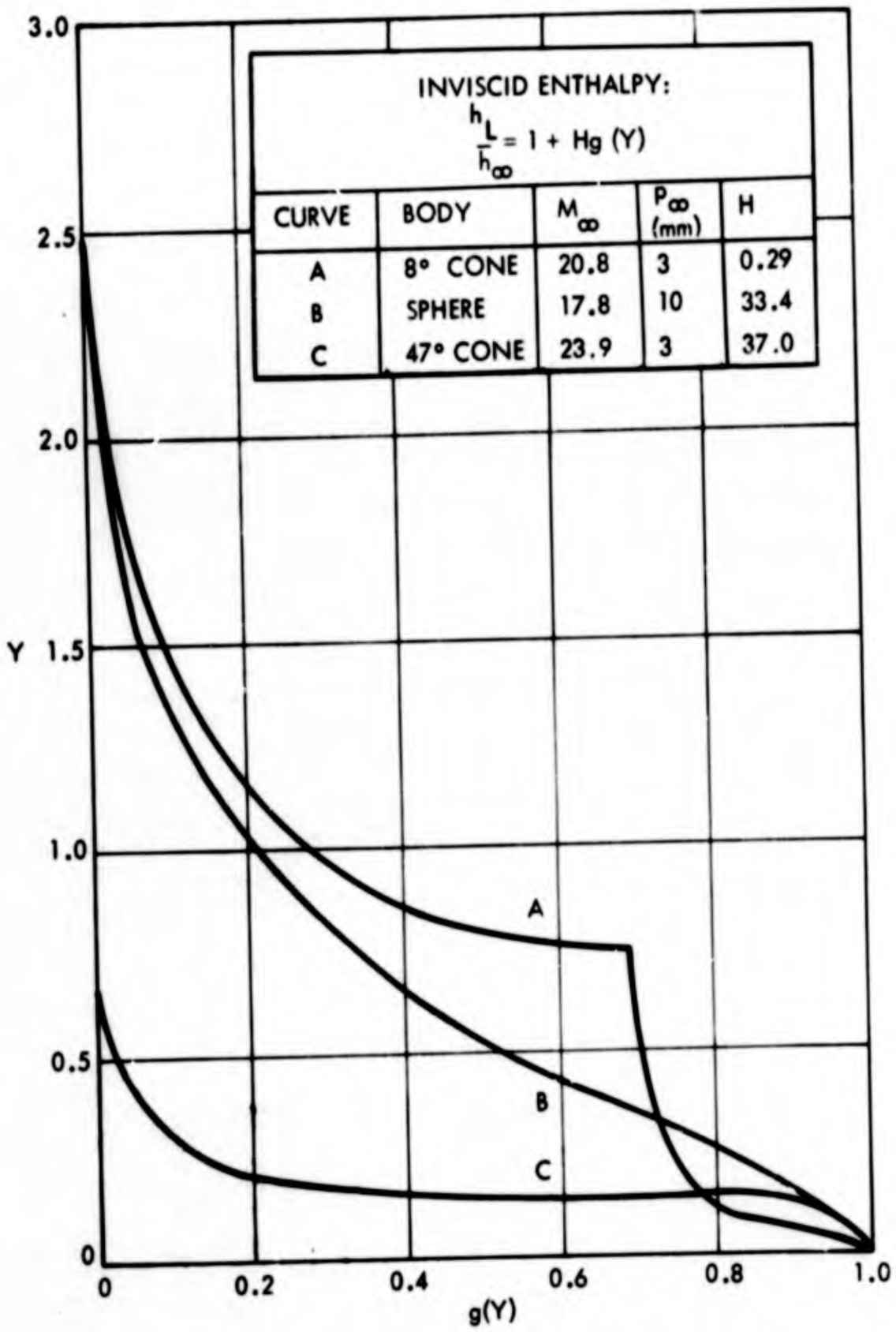

Figure 1. Inviscid Enthalpy Distribution

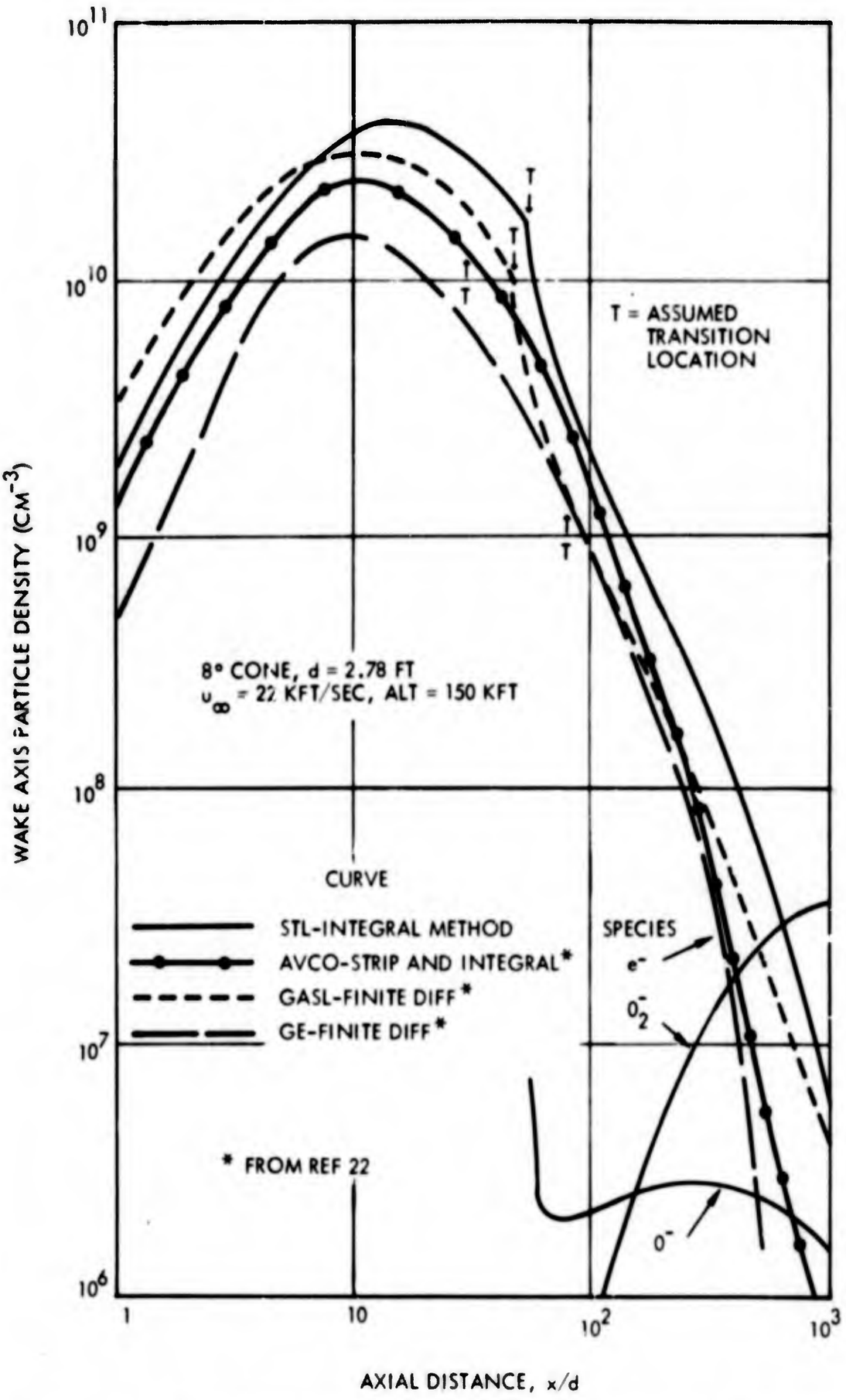

Figure 2. Wake Axis Electron Density - Comparison of Theories For Slender Cone

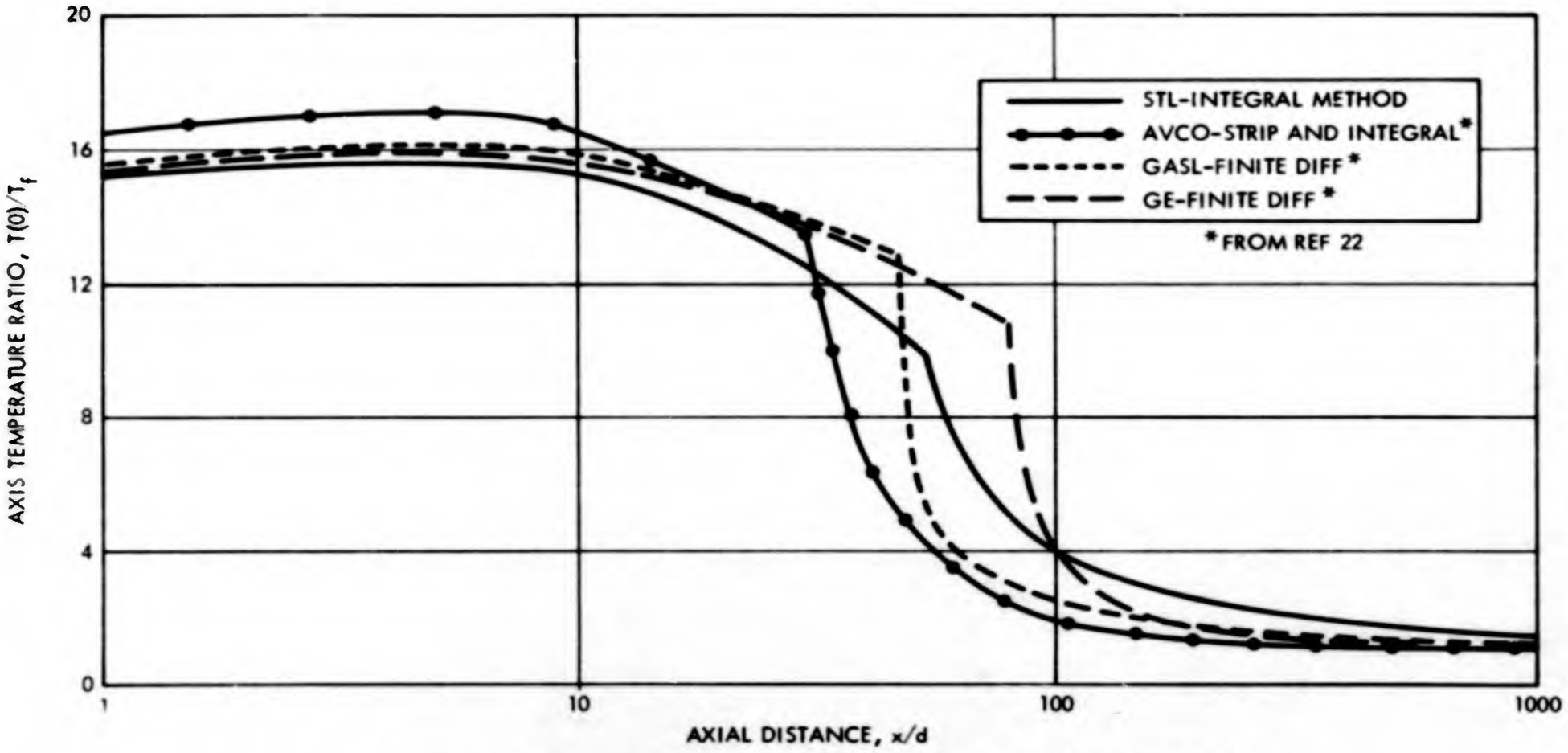

Figure 3. Wake Axis Temperature-Comparison of Theories for Slender Cone

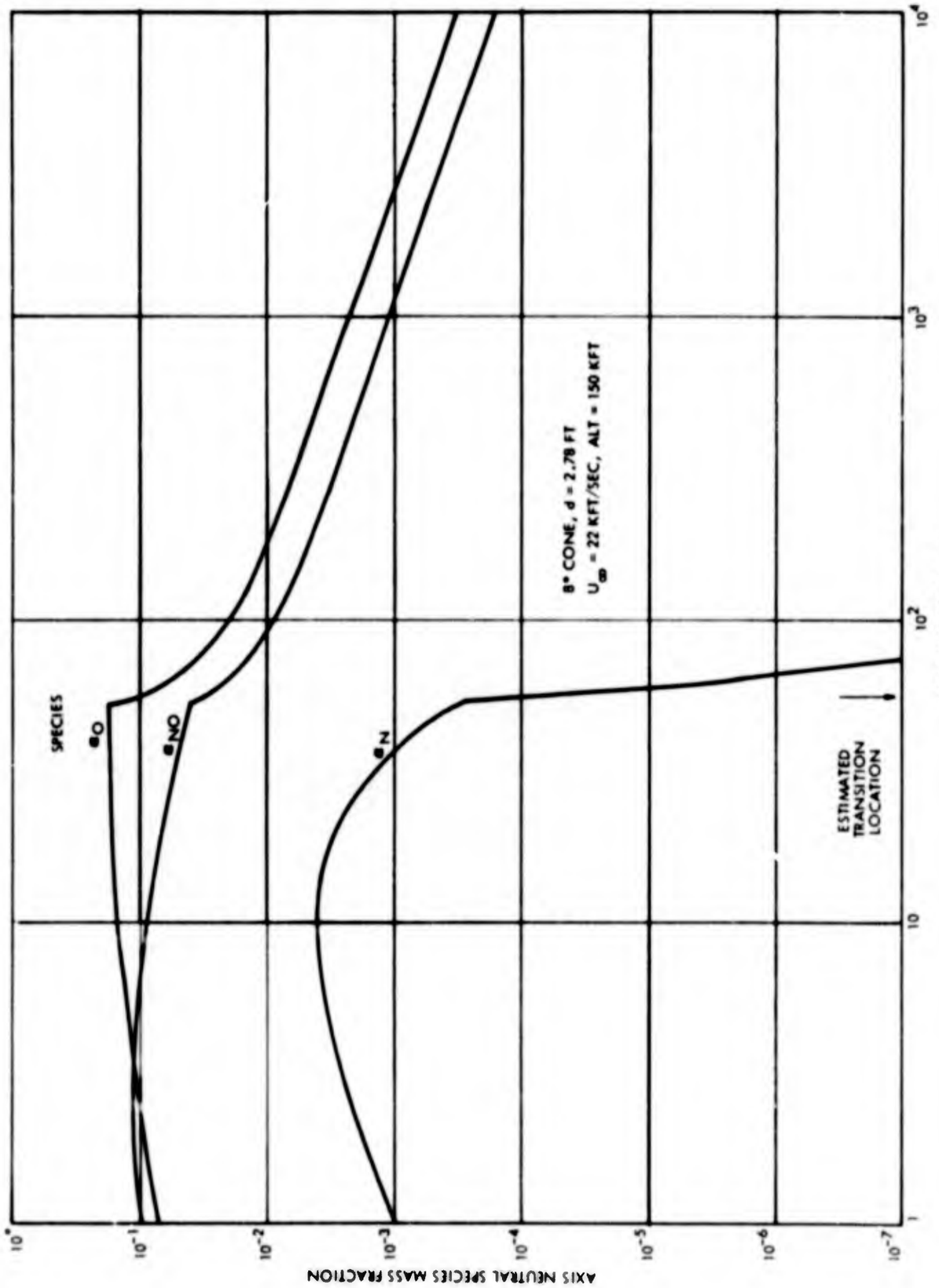

Figure 4. Neutral Species on Wake Axis-Slender Cone

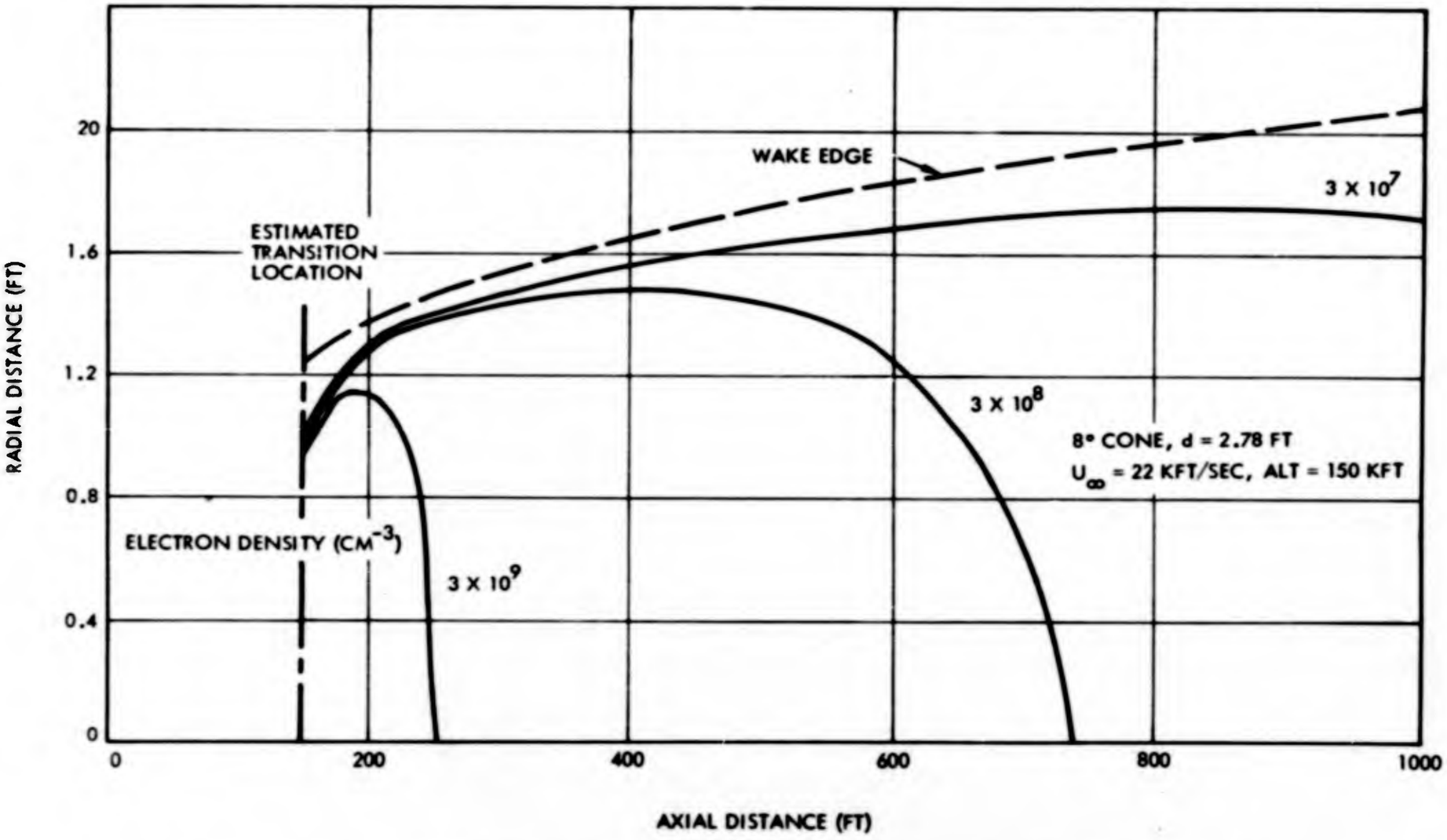

Figure 5. Mean Electron Density Contours For Turbulent Wake of Slender Cone

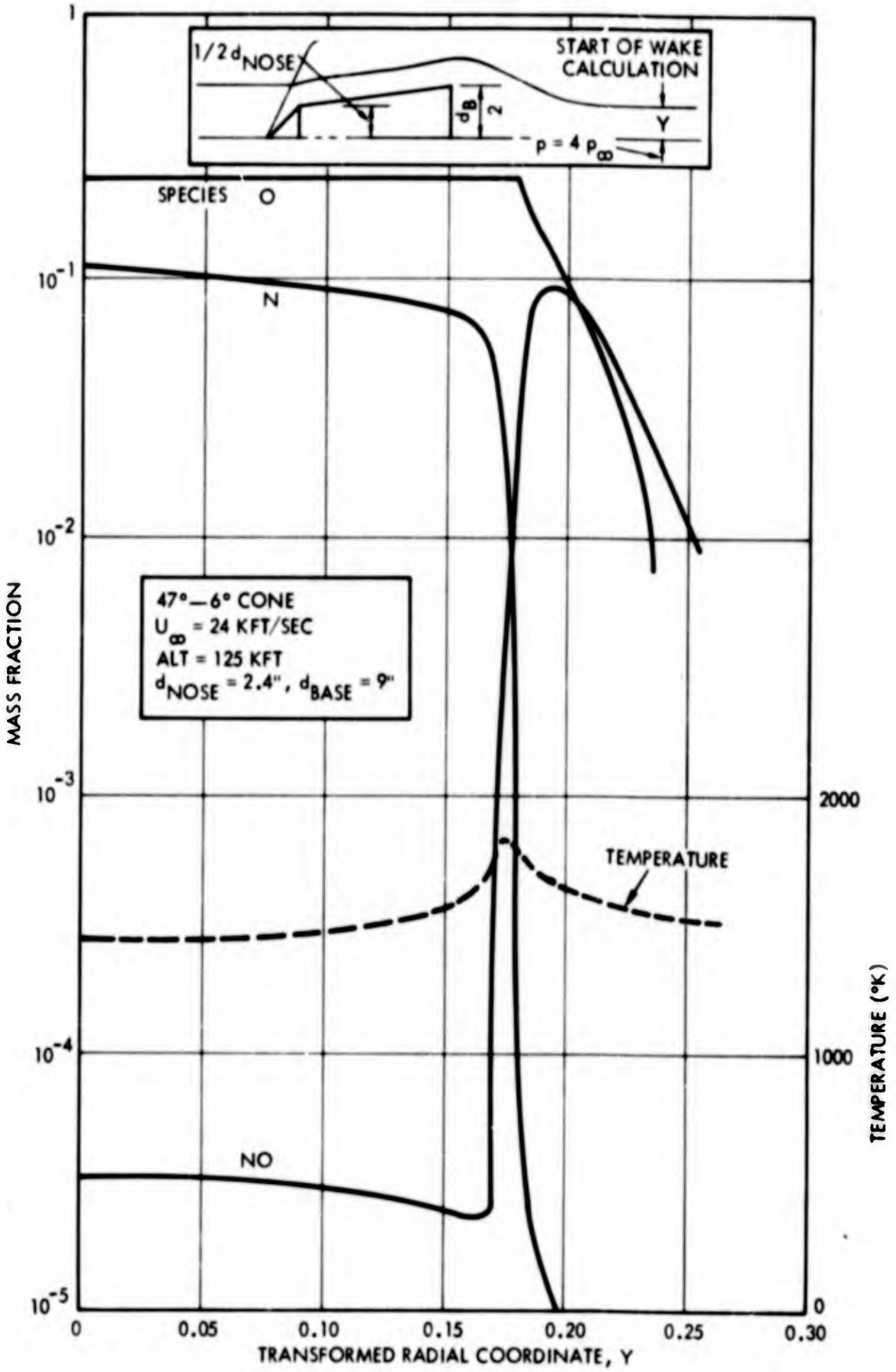

Figure 6. Non Equilibrium Species Mass Fractions and Temperature For Inviscid Flow at Initial Wake Station—Bi Conic Shape

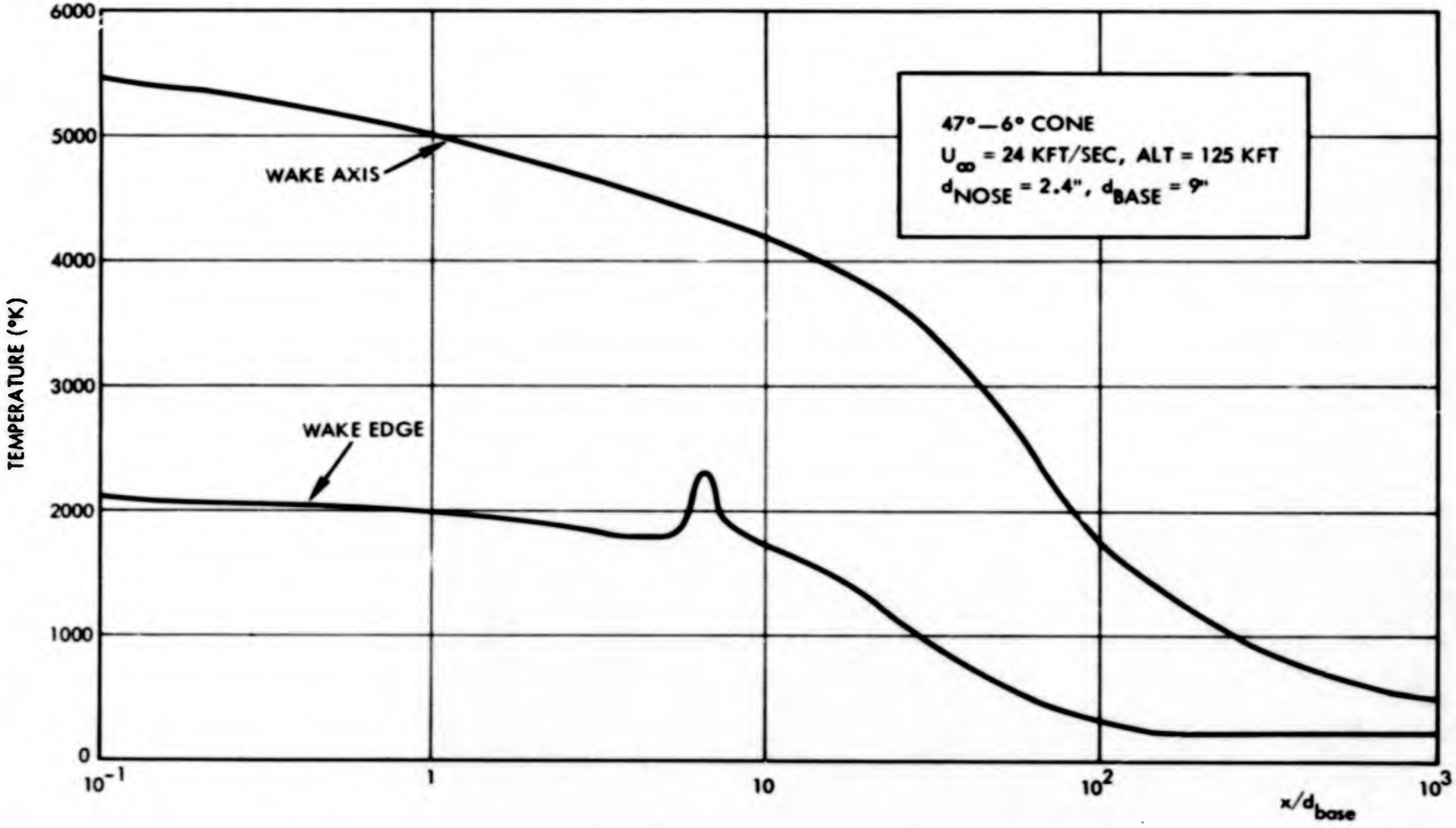

Figure 7. Axis and Wake Edge Temperature, Bi-Conic Shape

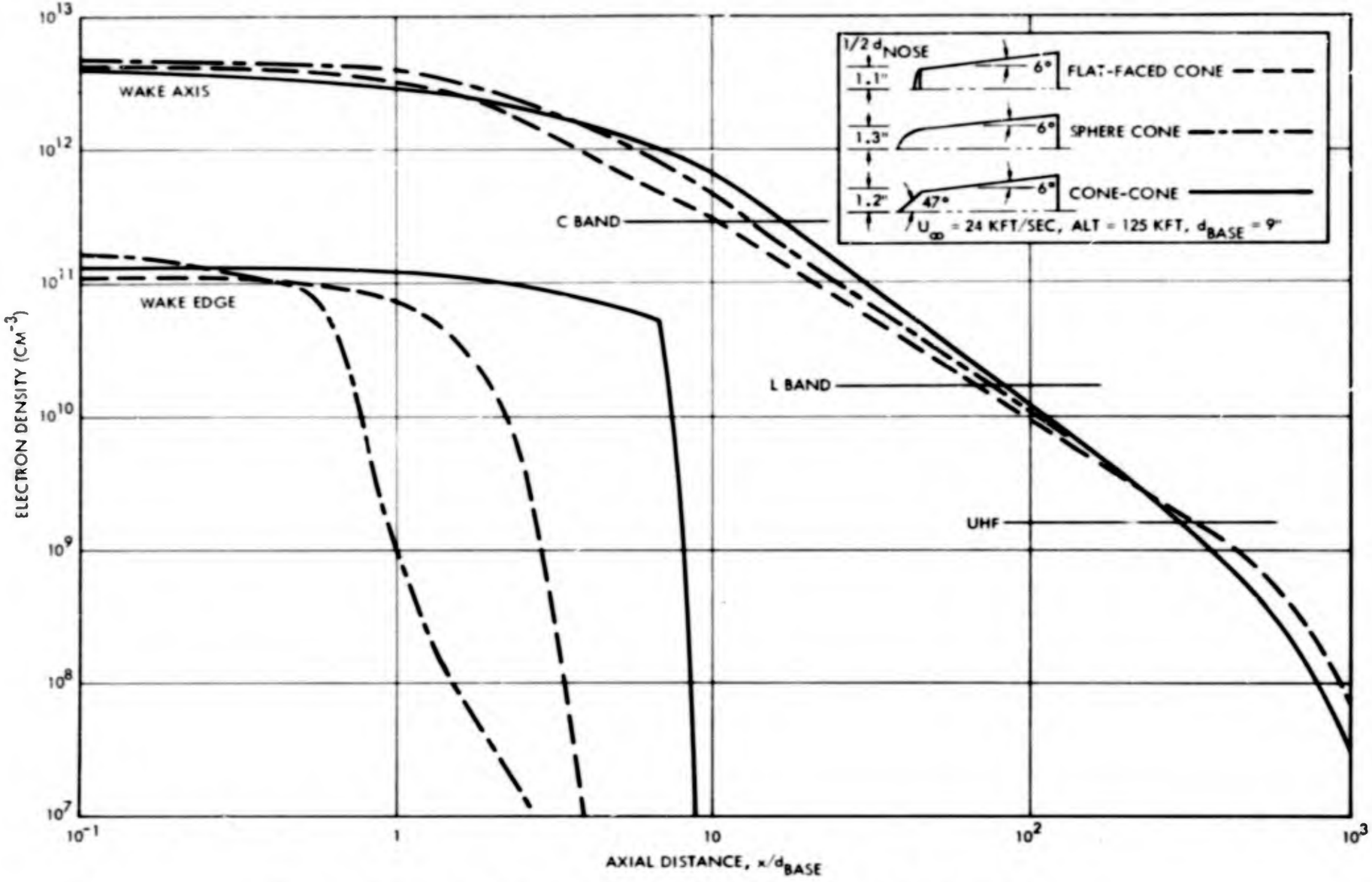

Figure 8. Wake Electron Densities For Several Blunt Cones

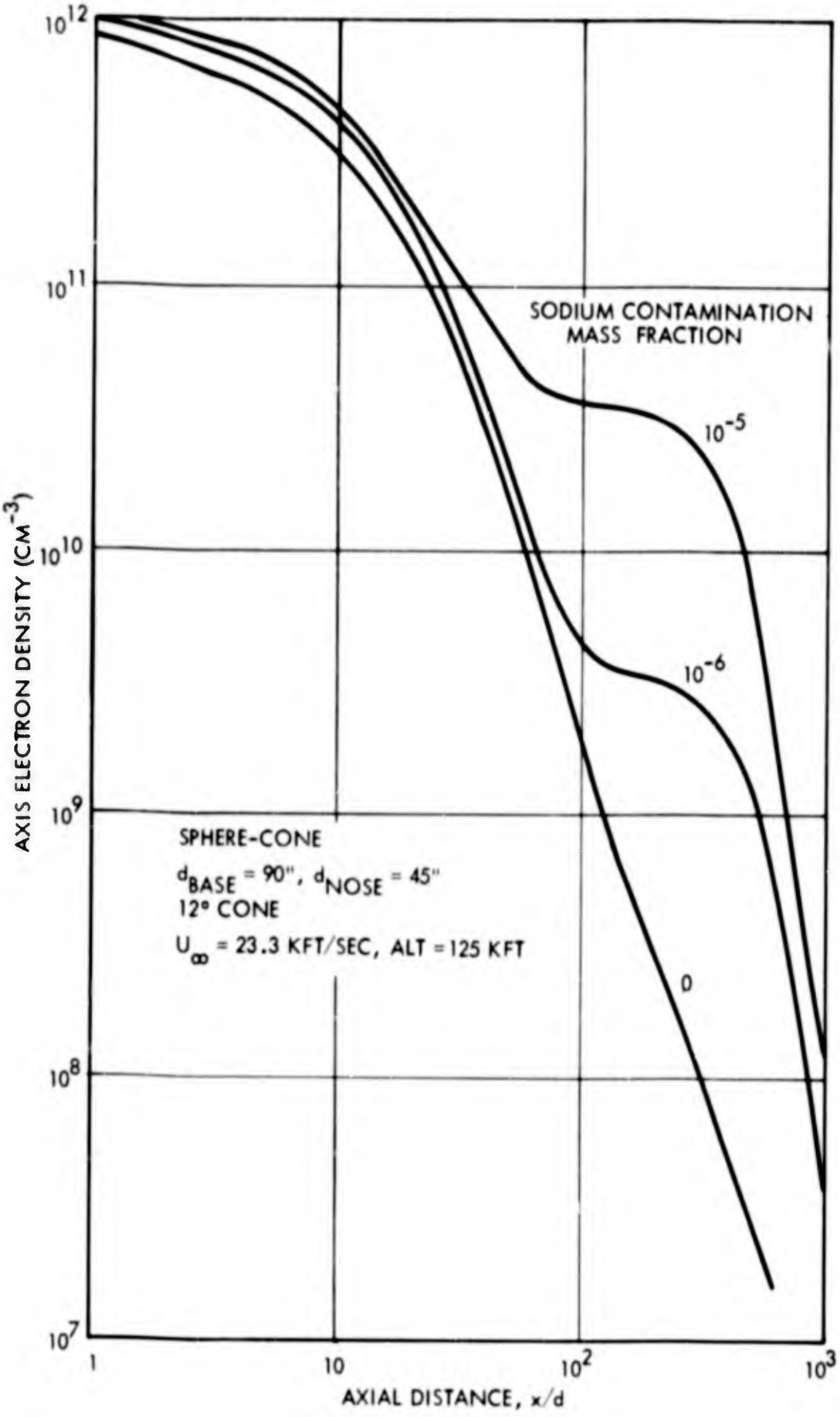

Figure 9A. Effect of Sodium Contamination on Electron Level of Turbulent Blunt Cone Wake

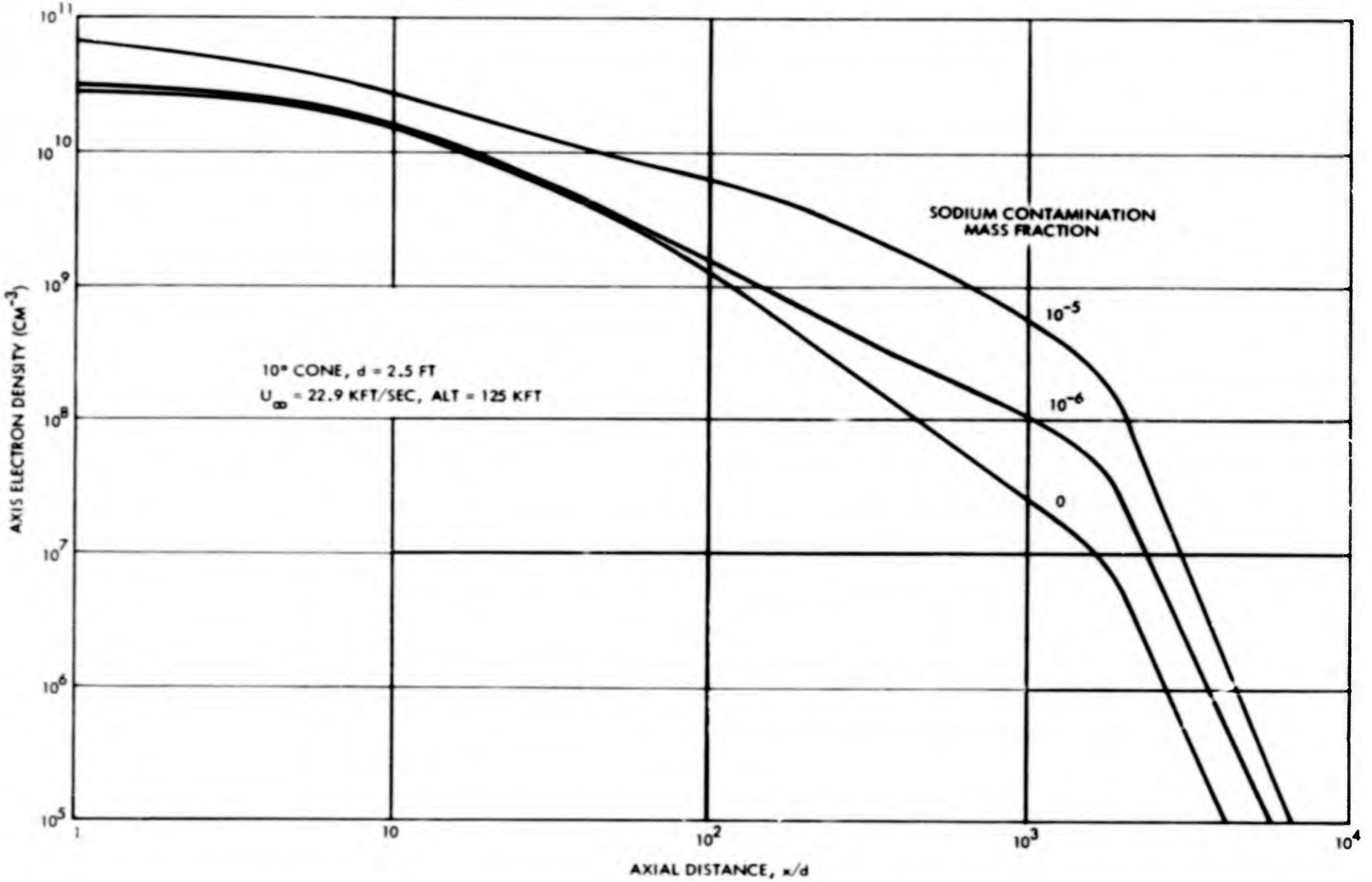

Figure 9B. Effect of Sodium Contamination on Electron Level of Turbulent Slender Cone Wake

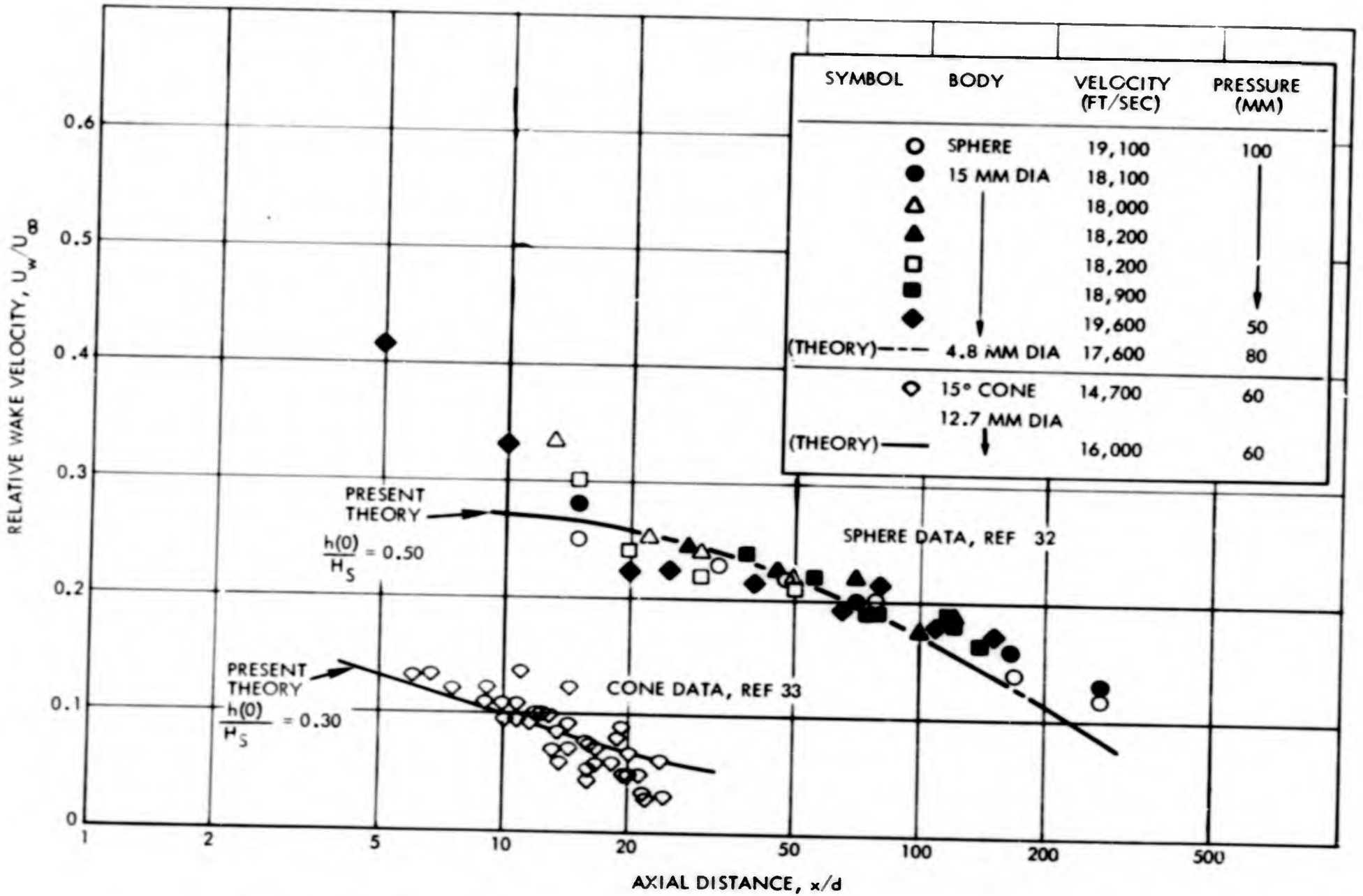

Figure 10. Wake Velocity — Comparison With Experimental Data

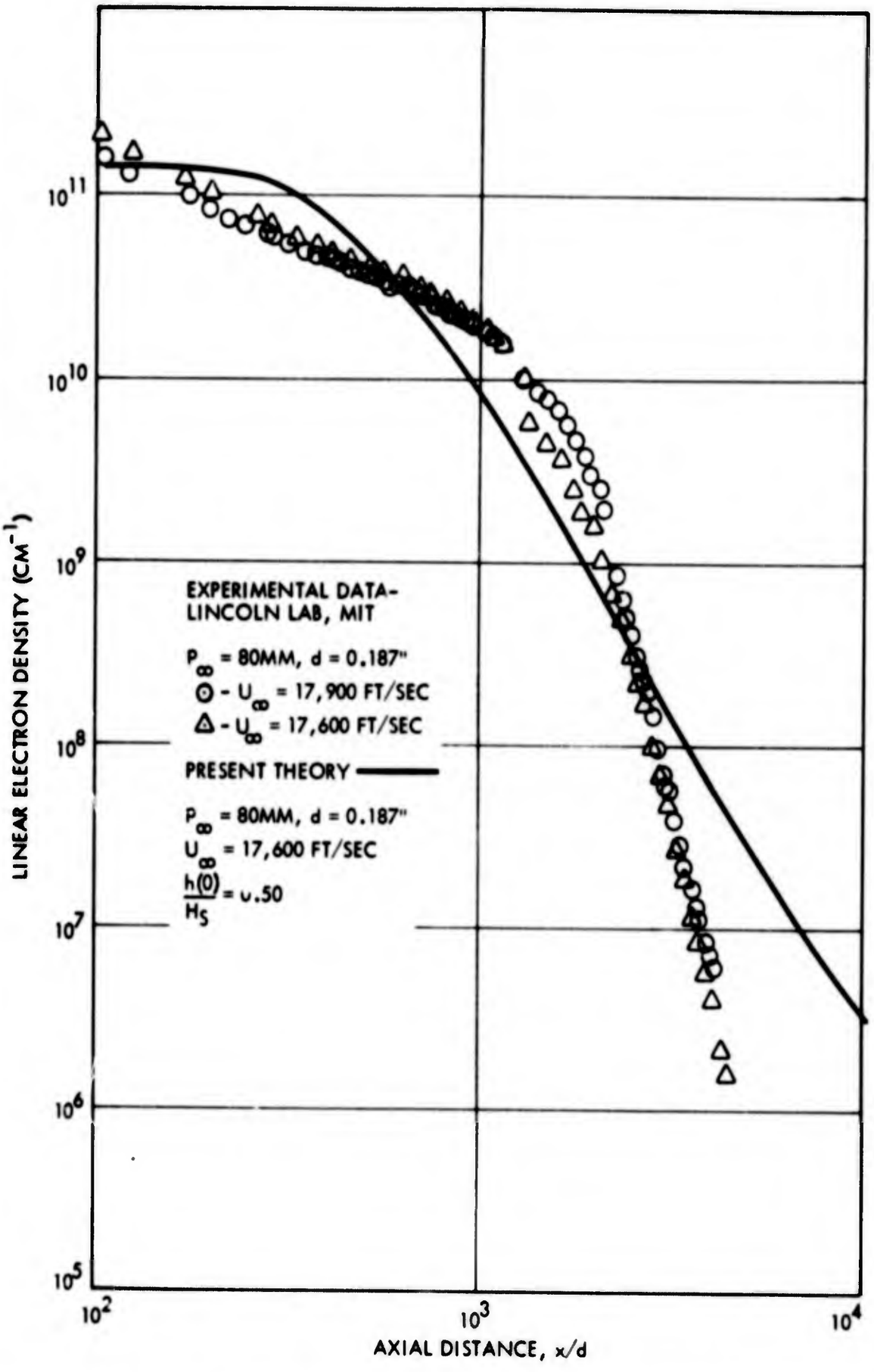

Figure 11A. Linear Electron Density — Comparison With Experiment

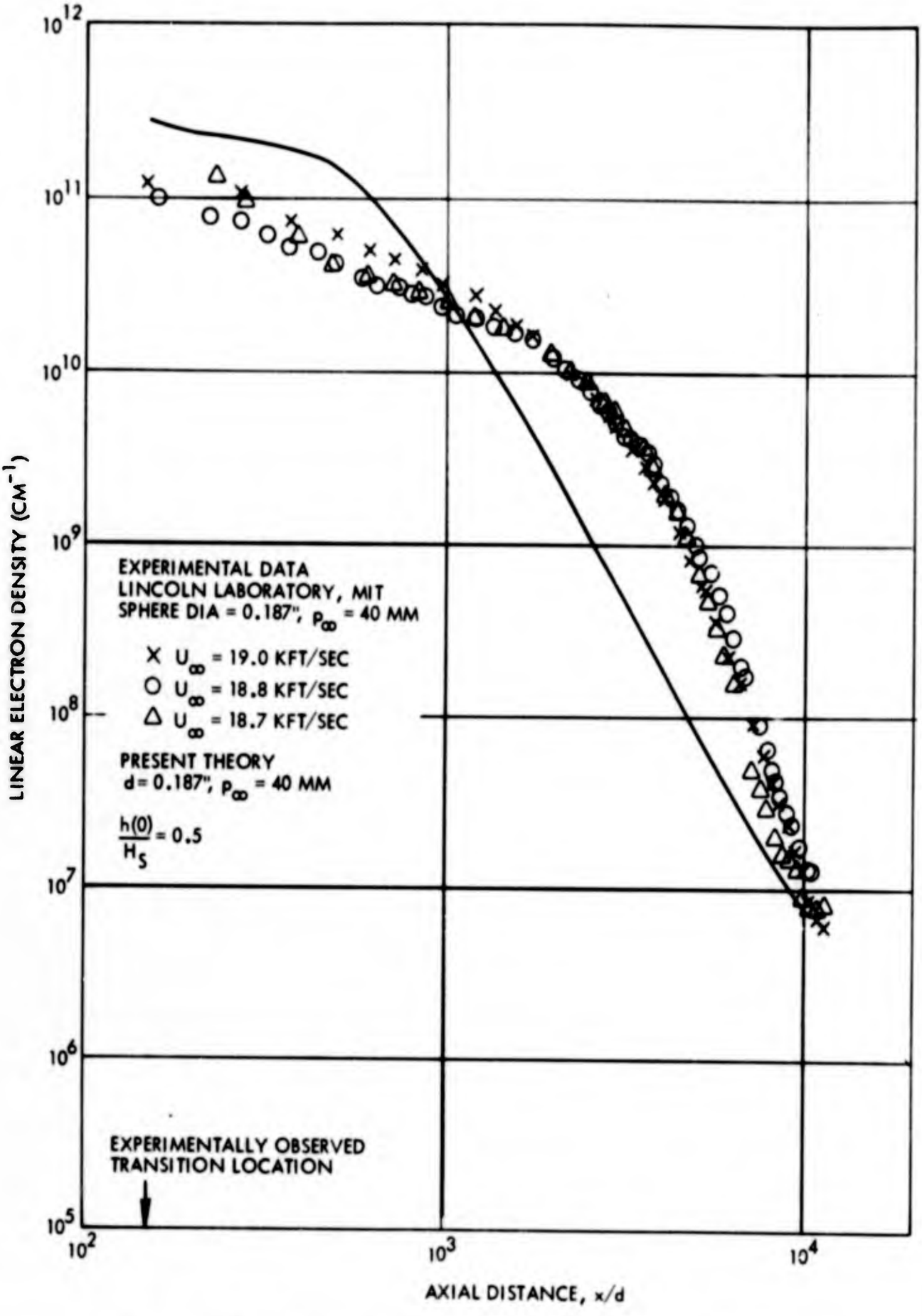

Figure 11B. Linear Electron Density — Comparison with Experiment (40 mm)

Unclassified

Security Classification

DOCUMENT CONTROL DATA - R&D

(Security classification of title, body of abstract and indexing annotation must be entered when the overall report is classified)

1 ORIGINATING ACTIVITY (Corporate author)

TRW Space Technology Laboratories
One Space Park - Redondo Beach, California

2a REPORT SECURITY CLASSIFICATION

Unclassified

2b GROUP --

3 REPORT TITLE

Turbulent Diffusion of a Reacting Wake

4 DESCRIPTIVE NOTES (Type of report and inclusive dates)

Technical Note

5 AUTHOR(S) (Last name, first name, initial)

Webb, Wilmot H. and Hromas, Leslie A.

6 REPORT DATE	7a TOTAL NO. OF PAGES	7b NO. OF REFS
January 30, 1964-Revised 12/3/64	41	38

8a CONTRACT OR GRANT NO.	9a ORIGINATOR'S REPORT NUMBER(S)
AF04(694)-440	6453-6012-KU-000
b PROJECT NO.	
c	9b OTHER REPORT NO(S) (Any other numbers that may be assigned this report)
d	BSD-TR-64-342

10 AVAILABILITY/LIMITATION NOTICES

None

11 SUPPLEMENTARY NOTES	12 SPONSORING MILITARY ACTIVITY
	Ballistic Systems Division, AFSC Norton Air Force Base, California

13 ABSTRACT - Properties of the nonequilibrium hypersonic turbulent wake have been calculated from an integral solution for the coupled diffusion of mass and energy. Emphasis is placed on: 1) a comparison of a slender body calculation from the present simple method with results obtained for the same case by more advanced mathematical techniques such as finite difference methods, 2) new blunt body results in which the reacting inviscid flow is entrained by the turbulent inner wake, 3) the effect of contaminants on both slender and blunt body wakes, 4) a comparison of the present calculations with ballistic range measurements for wake velocity and electron density. The analysis described herein is a direct extension of the method proposed by Lees and Hromas for the equilibrium wake. By using two parameters to describe the distribution of each species in the wake, the integral method applied here provides sufficient generality to permit the determination of a variety of reacting turbulent flow fields, yet retains the basic numerical simplicity inherent in integral techniques. In the chemical kinetic model studied, particular attention is paid to the processes of far downstream electron decay, and for the first time combined atomic and molecular oxygen attachment, charge neutralization, and charge exchange reactions are considered. In addition, some new explicit solutions are given which provide useful criteria in evaluating the respective role of chemical reactions and diffusion in the wake. These solutions are useful in obtaining scaling laws which are not always evident in detailed computer calculations.

DD FORM 1 JAN 64 1473

Unclassified

Security Classification

14 KEY WORDS	LINK A		LINK B		LINK C	
	ROLE	WT	ROLE	WT	ROLE	WT

INSTRUCTIONS

1. **ORIGINATING ACTIVITY**: Enter the name and address of the contractor, subcontractor, grantee, Department of Defense activity or other organization *(corporate author)* issuing the report.

2a. **REPORT SECURITY CLASSIFICATION**: Enter the overall security classification of the report. Indicate whether "Restricted Data" is included. Marking is to be in accordance with appropriate security regulations.

2b. **GROUP**: Automatic downgrading is specified in DoD Directive 5200.10 and Armed Forces Industrial Manual. Enter the group number. Also, when applicable, show that optional markings have been used for Group 3 and Group 4 as authorized.

3. **REPORT TITLE**: Enter the complete report title in all capital letters. Titles in all cases should be unclassified. If a meaningful title cannot be selected without classification, show title classification in all capitals in parenthesis immediately following the title.

4. **DESCRIPTIVE NOTES**: If appropriate, enter the type of report, e.g., interim, progress, summary, annual, or final. Give the inclusive dates when a specific reporting period is covered.

5. **AUTHOR(S)**: Enter the name(s) of author(s) as shown on or in the report. Enter last name, first name, middle initial. If military, show rank and branch of service. The name of the principal author is an absolute minimum requirement.

6. **REPORT DATE**: Enter the date of the report as day, month, year, or month, year. If more than one date appears on the report, use date of publication.

7a. **TOTAL NUMBER OF PAGES**: The total page count should follow normal pagination procedures, i.e., enter the number of pages containing information.

7b. **NUMBER OF REFERENCES**: Enter the total number of references cited in the report.

8a. **CONTRACT OR GRANT NUMBER**: If appropriate, enter the applicable number of the contract or grant under which the report was written.

8b, 8c, & 8d. **PROJECT NUMBER**: Enter the appropriate military department identification, such as project number, subproject number, system numbers, task number, etc.

9a. **ORIGINATOR'S REPORT NUMBER(S)**: Enter the official report number by which the document will be identified and controlled by the originating activity. This number must be unique to this report.

9b. **OTHER REPORT NUMBER(S)**: If the report has been assigned any other report numbers *(either by the originator or by the sponsor)*, also enter this number(s).

10. **AVAILABILITY/LIMITATION NOTICES**: Enter any limitations on further dissemination of the report, other than those imposed by security classification, using standard statements such as:

(1) "Qualified requesters may obtain copies of this report from DDC."

(2) "Foreign announcement and dissemination of this report by DDC is not authorized."

(3) "U. S. Government agencies may obtain copies of this report directly from DDC. Other qualified DDC users shall request through _____."

(4) "U. S. military agencies may obtain copies of this report directly from DDC. Other qualified users shall request through _____."

(5) "All distribution of this report is controlled. Qualified DDC users shall request through _____."

If the report has been furnished to the Office of Technical Services, Department of Commerce, for sale to the public, indicate this fact and enter the price, if known.

11. **SUPPLEMENTARY NOTES**: Use for additional explanatory notes.

12. **SPONSORING MILITARY ACTIVITY**: Enter the name of the departmental project office or laboratory sponsoring *(paying for)* the research and development. Include address.

13. **ABSTRACT**: Enter an abstract giving a brief and factual summary of the document indicative of the report, even though it may also appear elsewhere in the body of the technical report. If additional space is required, a continuation sheet shall be attached.

It is highly desirable that the abstract of classified reports be unclassified. Each paragraph of the abstract shall end with an indication of the military security classification of the information in the paragraph, represented as *(TS)*, *(S)*, *(C)*, or *(U)*.

There is no limitation on the length of the abstract. However, the suggested length is from 150 to 225 words.

14. **KEY WORDS**: Key words are technically meaningful terms or short phrases that characterize a report and may be used as index entries for cataloging the report. Key words must be selected so that no security classification is required. Identifiers, such as equipment model designation, trade name, military project code name, geographic location, may be used as key words but will be followed by an indication of technical context. The assignment of links, rules, and weights is optional.

BLANK PAGE